Eur. Phys. J. C 40, 165–186 (2005)
Digital Object Identifier (DOI) 10.1140/epjc/s2005-02141-1

THE EUROPEAN PHYSICAL JOURNAL C

# Renormalization-group improved calculation of the $B \to X_s\gamma$ branching ratio

M. Neubert

Institute for High-Energy Phenomenology, Newman Laboratory for Elementary-Particle Physics, Cornell University, Ithaca, NY 14853, USA

Received: 18 September 2004 / Revised version: 18 January 2005 /
Published online: 21 February 2005 – © Springer-Verlag / Società Italiana di Fisica 2005

**Abstract.** Using results on soft-collinear factorization for inclusive $B$-meson decay distributions, a systematic study of the partial $B \to X_s\gamma$ decay rate with a cut $E_\gamma \geq E_0$ on photon energy is performed. For values of $E_0$ below about 1.9 GeV, the rate can be calculated without reference to shape functions using a multi-scale operator product expansion (MSOPE). The transition from the shape-function region to the MSOPE region is studied analytically. The resulting prediction for the $B \to X_s\gamma$ branching ratio depends on three large scales: $m_b$, $\sqrt{m_b\Delta}$, and $\Delta = m_b - 2E_0$. Logarithms associated with these scales are resummed at next-to-next-to-leading logarithmic order. While power corrections in $\Lambda_{\rm QCD}/\Delta$ turn out to be small, the sensitivity to the scale $\Delta \approx 1.1\,\text{GeV}$ (for $E_0 \approx 1.8\,\text{GeV}$) introduces significant perturbative uncertainties, which so far have been ignored. The new theoretical prediction for the $B \to X_s\gamma$ branching ratio with $E_\gamma \geq 1.8\,\text{GeV}$ is $\text{Br}(B \to X_s\gamma) = (3.38^{+0.31}_{-0.42} \pm 0.31) \times 10^{-4}$, where the first error is an estimate of perturbative uncertainties and the second one reflects uncertainties in input parameters. With this cut $(89^{+6}_{-7} \pm 1)\%$ of all events are contained. When this fraction is combined with the previously best prediction for the total decay rate, one obtains $\text{Br}(B \to X_s\gamma) = (3.30^{+0.31}_{-0.35} \pm 0.17) \times 10^{-4}$, with a somewhat less conservative estimate of parametric uncertainties. The implications of larger theory uncertainties for new physics searches are briefly explored with the example of the type-II two-Higgs-doublet model, for which the lower bound on the charged-Higgs mass is reduced compared with previous estimates to approximately 200 GeV at 95% confidence level.

## 1 Introduction

The inclusive, weak radiative decay $B \to X_s\gamma$ is the prototype of all flavor-changing neutral current processes. In the standard model, this process is mediated by loop diagrams containing $W$ bosons and top (or lighter) quarks. In extensions of the standard model, other heavy particles propagating in loops can give sizable contributions, which in many cases can compete with those of the standard model. As a result, measurements of the $B \to X_s\gamma$ rate and $CP$ asymmetry provide sensitive probes for new physics at the TeV scale. In many cases, the fact that these measurements agree with standard model predictions imposes non-trivial constraints on the allowed parameter space.

Given the prominent role of $B \to X_s\gamma$ decay in searching for physics beyond the standard model, it is of great importance to have a precise prediction for its inclusive rate and $CP$ asymmetry in the standard model. This has been achieved thanks to the combined effort of many theorists over a period of several years [1]. The total inclusive rate is known at next-to-leading order in renormalization-group (RG) improved perturbation theory with a theoretical precision of about 10%. Currently, a major effort is underway to improve this accuracy by calculating the dominant parts of the next-to-next-to-leading corrections [2,3].

While the total inclusive $B \to X_s\gamma$ decay rate can be calculated using a conventional operator-product expansion (OPE) based on an expansion in logarithms and inverse powers of the $b$-quark mass [4], the situation is more complicated when a cut on the photon energy is applied. In practice, experiments can only measure the high-energy part of the photon spectrum, $E_\gamma \geq E_0$, where typically $E_0 = 2\,\text{GeV}$ (measured in the $B$-meson rest frame) or slightly lower [5,6]. Even if such a cut was not required for experimental reasons, it would be needed to reduce the photon background from $B \to X_s\psi^{(\prime)}$ decays followed by a radiative decay of the $\psi^{(\prime)}$ [7]. With $E_\gamma$ restricted to be close to the kinematic endpoint at $M_B/2$ (neglecting the kaon mass), the hadronic final state $X_s$ is constrained to have large energy $E_X \sim M_B$ but only moderate invariant mass $M_X \sim (M_B\Lambda_{\rm QCD})^{1/2}$. In this kinematic region, important hadronic effects need to be taken into account. An infinite set of leading-twist terms in the OPE need to be resummed into a non-perturbative shape function, which describes the momentum distribution of the $b$-quark inside the $B$ meson [8–10]. In addition, Sudakov double logarithms arise near the endpoint of the photon spectrum, which need to be resummed to all orders in perturbation theory [11–13]. While these issues are now well understood theoretically [14,15], the presence of the shape function

leads to an unavoidable element of hadronic uncertainty and modeling, which is undesirable when the goal is to probe for physics beyond the standard model.

Conventional wisdom says that, while shape-function effects are important near the endpoint of the photon spectrum, these effects can be ignored as soon as the cutoff $E_0$ is lowered below about 1.9 GeV. This assumption is based on phenomenological studies of shape-function effects using various model functions, which have the unrealistic feature that the distribution function vanishes exponentially for large light-cone momenta [16, 17]. In other words, it has been implicitly assumed that there is an instantaneous transition from the "shape-function region" of large non-perturbative corrections to the "OPE region", in which hadronic corrections to the rate are suppressed by at least two powers of $\Lambda_{\rm QCD}/m_b$. As a result, the preferred strategy has been to encourage experimenters to lower the photon-energy cut to a value $E_0 \le 1.9\,\text{GeV}$, and then to employ the conventional OPE for the calculation of the rate, ignoring shape-function effects.

In this paper we show that this strategy is based on a misconception. Our work is motivated by two considerations. First, is has recently been shown that the asymptotic behavior of $B$-meson distribution functions such as the shape function is not exponential, but rather governed by radiative tails exhibiting a slow, power-like fall-off [14,18]. One should therefore not exclude the possibility of a significant radiation tail in the case of the $B \to X_s\gamma$ photon spectrum, meaning that more events than predicted by existing models could be located at low photon energy. Fits to experimental data in the low-energy part of the spectrum, which are based on such models, should thus be taken with caution. Secondly, it has been our desire for a long time to find an analytic way to study the transition from the shape-function region to the OPE region. If it were true that shape-function effects become irrelevant once the cutoff $E_0$ is lowered below 1.9 GeV, one should be able to see this analytically using some form of a short-distance expansion. We show that this expansion indeed exists, and that it involves three different short-distance scales. In addition to the hard scale $m_b$, an intermediate "hard-collinear" scale $\sqrt{m_b\Delta}$ corresponding to the typical invariant mass of the hadronic final state $X_s$, and a low scale $\Delta = m_b - 2E_0$ related to the width of the energy window over which the measurement is performed, become of crucial importance. The physics associated with these scales can be disentangled using recent results on soft-collinear factorization theorems derived in the framework of effective field theory [14, 15]. A systematic treatment consists of matching QCD onto soft-collinear effective theory (SCET) [19] in a first step, in which hard quantum fluctuations are integrated out. In a second step, hard-collinear modes are integrated out by matching SCET onto heavy-quark effective theory (HQET) [20]. Ultimately, the precision of the theoretical calculations is determined by the value of the lowest short-distance scale $\Delta$, which in practice is of order 1 GeV or only slightly larger. The theoretical accuracy that can be reached is therefore not as good as in the case of a conventional heavy-quark expansion applied to the $B$ system, but more likely it is similar to (if not worse than) the accuracy reached in the description of the inclusive hadronic $\tau$ decay rate $R_\tau$ [21]. However, while the ratio $R_\tau$ is known to order $\alpha_s^3$, the $B \to X_s\gamma$ branching ratio is currently only known through order $\alpha_s$.

While we are aware that this conclusion may come as a surprise to many practitioners in the field of flavor physics, we believe that it is an unavoidable consequence of the analysis presented in this paper. Not surprisingly, then, we find that the error estimates for the partial $B \to X_s\gamma$ branching ratio in the literature are too optimistic. Since there are unknown $\alpha_s^2(\Delta)$ corrections at the low scale $\Delta \sim 1\,\text{GeV}$, we estimate the present perturbative uncertainty in the $B \to X_s\gamma$ branching ratio with $E_0$ in the range between 1.6 and 1.8 GeV to be of order 10%. In addition, there are uncertainties due to other sources, such as the $b$- and $c$-quark masses. The combined theoretical uncertainty is of order 15%. While this is a rather pessimistic conclusion, we stress that the uncertainty is limited by unknown, higher-order perturbative terms, not by non-perturbative effects, which we find to be under good control. (This is similar to the case of $R_\tau$.) Therefore, there is room for a reduction of the error by means of well-controlled perturbative calculations.

In Sect. 2, we discuss the QCD factorization formula for the partial $B \to X_s\gamma$ decay rate with a cut $E_\gamma \ge E_0$ on photon energy, valid at leading power in the heavy-quark expansion. Contributions associated with the hard, hard-collinear, and soft scales are factorized into a hard function $H_\gamma$, a jet function $J$, and a shape function $\hat{S}$. Single and double (Sudakov) logarithms are systematically resummed to all orders in perturbation theory. The RG evolution of the shape function is studied in Sect. 3, where we present the exact solution to its evolution equation in momentum space. Our main results are derived in Sect. 4, where we show how the convolution integral over the shape function in the factorization formula can be calculated using a local OPE, provided that the scale $\Delta = m_b - 2E_0$ is numerically large compared with $\Lambda_{\rm QCD}$. Section 5 discusses how to eliminate the HQET parameters $m_b$ and $\lambda_1$ defined in the pole scheme, which enter the theoretical expressions, in terms of physical parameters defined in the so-called "shape-function scheme" [14]. The calculation of the decay rate is completed in Sect. 6, where we add contributions that are power-suppressed in the heavy-quark expansion. For these small corrections, the scale separation we achieve is only approximate and misses some yet unknown terms of order $\alpha_s^2 \ln^2(\Delta/m_b)$. In Sect. 7, we show that by considering ratios of decay rates one may separate the short-distance physics contained in the hard function $H_\gamma$ from the physics associated with the intermediate and low scales. For instance, at leading power in $\Delta/m_b$ the ratio of the $B \to X_s\gamma$ branching ratio in a new physics model relative to that in the standard model can be calculated without any sensitivity to scales less than the hard scale $\mu_h \sim m_b$, and the same is true for the direct $CP$ asymmetry. In other cases, at leading power some ratios are insensitive to the Wilson coefficients in the effective weak Hamiltonian and thus to new physics. Examples are the average photon

energy $\langle E_\gamma \rangle$, and the ratio of the $B \to X_s\gamma$ decay rate with $E_\gamma \geq E_0$ normalized to the total rate. The latter ratio is particularly interesting, since it can be used to make contact between a simple, fully inclusive rate calculation and our more sophisticated analysis of multi-scale effects. Our numerical results are presented in Sect. 8, followed by a summary and conclusions.

## 2 QCD factorization theorem

Recent results on the factorization of hard, hard-collinear, and soft contributions to inclusive $B$-meson decay distributions [14, 15] allow us to obtain a QCD factorization formula for the integrated $B \to X_s\gamma$ decay rate with a cut $E_\gamma \geq E_0$ on photon energy. In the region of large $E_0$, the leading contribution to the rate can be written in the form

$$\begin{aligned}
&\Gamma_{\bar B\to X_s\gamma}(E_0)\\
&= \frac{G_{\rm F}^2\alpha}{32\pi^4}\,|V_{tb}V_{ts}^*|^2\,(1+\varepsilon_{\rm np})\,\overline{m}_b^2(\mu_h)\,|H_\gamma(\mu_h)|^2\\
&\quad\times U_1(\mu_h,\mu_{\rm i})\int_0^{\Delta_E}{\rm d}P_+\,(M_B-P_+)^3\\
&\quad\times\int_0^{P_+}{\rm d}\hat\omega\,m_b\,J\big(m_b(P_+-\hat\omega),\mu_{\rm i}\big)\,\hat S(\hat\omega,\mu_{\rm i})\\
&\qquad+\text{power corrections},
\end{aligned}\tag{1}$$

where $\Delta_E = M_B - 2E_0$ is twice the width of the window in photon energy over which the measurement of the decay rate is performed. In the prefactor, $\alpha$ is the fine-structure constant normalized at $q^2 = 0$ [22]. The variable $P_+ = E_X - |\boldsymbol{P}_X|$ is the "plus component" of the four-momentum of the hadronic final state $X_s$, which is related to the photon energy by $P_+ = M_B - 2E_\gamma$. The factor $(M_B - P_+)^3$ under the integral thus equals $8E_\gamma^3$, where two powers of $E_\gamma$ come from the squared matrix element of the effective weak Hamiltonian, and one factor comes from phase space. The hadronic invariant mass of the final state is $M_X^2 = M_B P_+$. The endpoint region of the photon spectrum is defined by the requirement that $P_+ \leq \Delta_E \ll M_B$, in which case $P^\mu$ is called a hard-collinear momentum [23]. Power corrections to the expression above will be analyzed later; however, the leading non-perturbative corrections to the total decay rate have already been factored out in (1) and included in the parameter [4] (see Table 1 in Sect. 8 for a list of input parameters)

$$\varepsilon_{\rm np} = \frac{\lambda_1 - 9\lambda_2}{2m_b^2} = -(3.1\pm0.5)\%\,. \tag{2}$$

The factorization formula (1) was first presented in [12]. What is new is that we now have a systematic effective field-theory technology to compute the functions $H_\gamma$ and $J$ order by order in perturbation theory, and to control their scale dependence in momentum space (not moment space). Also, it is in principle possible to include power-suppressed terms in the heavy-quark expansion. In the factorization formula, $\mu_h \sim m_b$ is a hard scale, while $\mu_{\rm i} \sim \sqrt{m_b\Lambda_{\rm QCD}}$ is an intermediate hard-collinear scale of order the invariant mass of the hadronic final state. The precise values of these matching scales are irrelevant, since the rate is formally independent of $\mu_h$ and $\mu_{\rm i}$. The hard corrections captured by the function $H_\gamma(\mu_h)$ result from the matching of the effective weak Hamiltonian of the standard model (or any of its extensions) onto a leading-order current operator of SCET. It is defined by the relation

$$\begin{aligned}
\mathcal{H}_{\rm eff}^{b\to s\gamma} \to \frac{G_{\rm F}}{\sqrt{2}}\,V_{tb}V_{ts}^*\,\frac{e}{2\pi^2}\,E_\gamma\,\overline{m}_b(\mu_h)\,H_\gamma(\mu_h)\,\epsilon_\mu^*(q)\\
\times\big[\bar\xi\,W_{hc}\,\gamma_\perp^\mu(1-\gamma_5)\,h_v\big](\mu_h)+\dots\,,
\end{aligned}\tag{3}$$

where $\epsilon(q)$ is the transverse photon polarization vector, and the dots represent power-suppressed contributions from higher-dimensional SCET operators. The result is proportional to the photon energy, $E_\gamma = v\cdot q$, defined in the $B$-meson rest frame. (Here $v$ is the 4-velocity of the $B$ meson.) The fields $h_v$ and $\xi$ represent the soft heavy quark and the hard-collinear strange quark, respectively, and $W_{hc}$ is a Wilson line. At tree level, only the dipole operator $Q_{7\gamma}$ and the four-quark penguin operators $Q_5$ and $Q_6$ in the effective weak Hamiltonian give a non-zero contribution to $H_\gamma$, which is equal to the "effective" coefficient $C_{7\gamma}^{\rm eff} = C_{7\gamma} - \frac{1}{3}\,C_5 - C_6$. (We use the conventions of [24] for the operators and Wilson coefficients in the effective weak Hamiltonian.) At next-to-leading order, the result reads (with $C_F = 4/3$)

$$\begin{aligned}
&H_\gamma(\mu_h)\\
&= C_{7\gamma}^{\rm eff}(\mu_h)\bigg[1\\
&\quad+\frac{C_F\alpha_{\rm s}(\mu_h)}{4\pi}\left(-2\ln^2\frac{m_b}{\mu_h}+7\ln\frac{m_b}{\mu_h}-6-\frac{\pi^2}{12}\right)+\varepsilon_{\rm ew}\bigg]\\
&\quad+C_{8g}^{\rm eff}(\mu_h)\,\frac{C_F\alpha_{\rm s}(\mu_h)}{4\pi}\\
&\quad\times\left(-\frac{8}{3}\ln\frac{m_b}{\mu_h}+\frac{11}{3}-\frac{2\pi^2}{9}+\frac{2\pi{\rm i}}{3}\right)\\
&\quad+C_1(\mu_h)\,\frac{C_F\alpha_{\rm s}(\mu_h)}{4\pi}\\
&\quad\times\left(\frac{104}{27}\ln\frac{m_b}{\mu_h}+g(z)+\varepsilon_{\rm CKM}\,\big[g(0)-g(z)\big]\right)\\
&\quad+\varepsilon_{\rm peng}\,.
\end{aligned}\tag{4}$$

The coefficient $C_{7\gamma}^{\rm eff}(\mu_h)$ of the electromagnetic dipole operator is required with next-to-leading order accuracy [25], while the remaining coefficients can be calculated at leading logarithmic order. Explicit expressions for these coefficients can be found, e.g., in [17, 25]. The terms in the third row arise from charm-quark and up-quark penguin contractions of the current–current operators $Q_1^{c,u}$. These contributions depend on the small ratio

$$\begin{aligned}
\varepsilon_{\rm CKM} &= -\frac{V_{ub}V_{us}^*}{V_{tb}V_{ts}^*}\\
&= \lambda^2(\bar\rho-{\rm i}\bar\eta)\,\big[1+\lambda^2(1-\bar\rho-{\rm i}\bar\eta)+\mathcal{O}(\lambda^4)\big]\,.
\end{aligned}\tag{5}$$

The variable $z = (m_c/m_b)^2$ denotes the ratio of quark masses relevant to the charm loop, and

$$\begin{aligned} g(z) &= -\frac{833}{162} - \frac{20\pi\mathrm{i}}{27} + \frac{8\pi^2}{9}\, z^{3/2} \\ &+ \frac{2z}{9}\left[48 - 5\pi^2 - 36\zeta_3 + (30\pi - 2\pi^3)\mathrm{i}\right. \\ &\left. + (36 - 9\pi^2 + 6\pi\mathrm{i})\ln z + (3 + 6\pi\mathrm{i})\ln^2 z + \ln^3 z\right] \\ &+ \frac{2z^2}{9}\left[18 + 2\pi^2 - 2\pi^3\mathrm{i} + (12 - 6\pi^2)\ln z\right. \\ &\left. + 6\pi\mathrm{i}\ln^2 z + \ln^3 z\right] \\ &+ \frac{z^3}{27}\left[-9 - 14\pi^2 + 112\pi\mathrm{i} + (182 - 48\pi\mathrm{i})\ln z\right. \\ &\left. - 126\ln^2 z\right] + \ldots \end{aligned} \tag{6}$$

are the first few terms in the expansion of the penguin function [26], whose exact expression (in the form of parameter integrals) can be found in [27]. The imaginary parts in (4) and (6) are strong-interaction phases, which in conjunction with $CP$-violating weak phases contained in the parameter $\varepsilon_{\rm CKM}$ or in potential new physics contributions to the Wilson coefficients can induce a non-zero $CP$ asymmetry in $B \to X_s\gamma$ decays [28, 29]. The term

$$\varepsilon_{\rm ew} = \delta_{\rm ew} + \frac{\alpha(\mu_h)}{\alpha_{\rm s}(\mu_h)}\, \frac{C_{7\gamma}^{(\rm em)}(\mu_h)}{C_{7\gamma}^{\rm eff}(\mu_h)} \approx -1.5\% \tag{7}$$

accounts for electroweak matching corrections at the weak scale [30] and logarithmically enhanced electromagnetic effects affecting the evolution of the Wilson coefficients [17, 31]. Finally, the term $\varepsilon_{\rm peng} \approx 0.2\%$ includes the effects of penguin contractions of operators other than $Q_1^{c,u}$ [27], which are numerically negligible but are included here for completeness. In the factorization formula (1), the hard function is multiplied by the running $b$-quark mass

$$\overline{m}_b(\mu_h) = \overline{m}_b(\overline{m}_b)\left[1 + \frac{3C_F\alpha_{\rm s}(\mu_h)}{2\pi}\,\ln\frac{\overline{m}_b}{\mu_h} + \ldots\right] \tag{8}$$

defined in the $\overline{\rm MS}$ scheme, which is part of the electromagnetic dipole operator $Q_{7\gamma}$. On the other hand, the scheme to be used for the quark masses entering the ratio $z$ in the penguin function $g(z)$ is not specified at next-to-leading order [7]. Since the matching is performed at a hard scale $\mu_h$, the charm-quark mass should be a running mass $\overline{m}_c(\mu_h)$, while $m_b$ enters either as the mass in the $b$-quark propagator or via the values of external momenta. For simplicity, we take $z = [\overline{m}_c(\mu_h)/\overline{m}_b(\mu_h)]^2$ as a ratio of running quark masses evaluated at the same scale, which has the advantage that this quantity is RG invariant.

The jet function $J\big(m_b(P_+ - \hat\omega), \mu_{\rm i}\big)$ in (1) describes the physics of the final-state hadronic jet. At next-to-leading order in perturbation theory, it is given by the expression [14, 15]

$$\begin{aligned} &m_b\, J\big(m_b(P_+ - \hat\omega), \mu_{\rm i}\big) \\ &= \delta(P_+ - \hat\omega)\left[1 + \frac{C_F\alpha_{\rm s}(\mu_{\rm i})}{4\pi}\left(7 - \pi^2\right)\right] \\ &\quad + \frac{C_F\alpha_{\rm s}(\mu_{\rm i})}{4\pi}\left[\frac{1}{P_+ - \hat\omega}\left(4\ln\frac{m_b(P_+ - \hat\omega)}{\mu_{\rm i}^2} - 3\right)\right]_*^{[\mu_{\rm i}^2/m_b]}. \end{aligned} \tag{9}$$

The star distributions are generalized plus distributions defined as [32]

$$\begin{aligned} &\int_{\le 0}^{z} {\rm d}x\, F(x)\left[\frac{1}{x}\right]_*^{[u]} \\ &= \int_0^z {\rm d}x\, \frac{F(x) - F(0)}{x} + F(0)\,\ln\frac{z}{u}\,, \\ &\int_{\le 0}^{z} {\rm d}x\, F(x)\left[\frac{\ln(x/u)}{x}\right]_*^{[u]} \\ &= \int_0^z {\rm d}x\, \frac{F(x) - F(0)}{x}\,\ln\frac{x}{u} + \frac{F(0)}{2}\,\ln^2\frac{z}{u}\,, \end{aligned} \tag{10}$$

where $F(x)$ is a smooth test function. The perturbative expansion of the jet function can be trusted as long as $\mu_{\rm i}^2 \sim m_b\Delta$ with $\Delta \sim P_+^{\rm max} - \langle\hat\omega\rangle \simeq m_b - 2E_0 \ll M_B$. By quark–hadron duality, only the maximum values of kinematic variables such as $P_+$, which are integrated over phase space, matter for the calculation of inclusive decay rates [4]. Note that the "natural" choices $\mu_h \propto m_b$ and $\mu_{\rm i}^2 \equiv m_b\,\tilde\mu_{\rm i}$ with $\tilde\mu_{\rm i}$ independent of $m_b$ remove all reference to the $b$-quark mass (other than in the arguments of running coupling constants) from the factorization formula (1).

The shape function $\hat S(\hat\omega, \mu_{\rm i})$ parameterizes our ignorance about the soft physics associated with bound-state effects inside the $B$ meson [8, 9]. Its naive interpretation is that of a parton distribution function, governing the distribution of the light-cone component $k_+$ of the residual momentum $k = p_b - m_b v$ of the $b$ quark inside the heavy meson. Once radiative corrections are included, however, a probabilistic interpretation of the shape function breaks down [14]. For convenience, the shape function is renormalized in (1) at the intermediate hard-collinear scale $\mu_{\rm i}$ rather than at a hadronic scale $\mu_{\rm had}$. This removes any uncertainties related to the evolution from $\mu_{\rm i}$ to $\mu_{\rm had}$. Since the shape function is universal, all that matters is that it is renormalized at the same scale when comparing different processes.

The last ingredient in the factorization formula (1) is the RG evolution function $U_1(\mu_h, \mu_{\rm i})$, which describes the evolution of the hard function $|H_\gamma|^2$ from the high matching scale $\mu_h$ down to the intermediate scale $\mu_{\rm i}$, at which the jet and shape functions are renormalized. The exact expression for this quantity follows from

$$\begin{aligned} &\ln U_1(\mu_h, \mu_{\rm i}) \\ &= 2S(\mu_h, \mu_{\rm i}) - 2a_\Gamma(\mu_h, \mu_{\rm i})\ln\frac{m_b}{\mu_h} - 2a_{\gamma'}(\mu_h, \mu_{\rm i})\,, \end{aligned} \tag{11}$$

where the various functions on the right-hand side are the solutions to the partial differential equations (the Sudakov exponent $S$ should not be confused with the shape function $\hat{S}$)

$$\begin{aligned}
\frac{\mathrm{d}}{\mathrm{d}\ln\mu}\, S(\nu,\mu) &= -\Gamma_{\rm cusp}\big(\alpha_{\rm s}(\mu)\big)\, \ln\frac{\mu}{\nu}\,, \\
\frac{\mathrm{d}}{\mathrm{d}\ln\mu}\, a_\Gamma(\nu,\mu) &= -\Gamma_{\rm cusp}\big(\alpha_{\rm s}(\mu)\big)\,, \\
\frac{\mathrm{d}}{\mathrm{d}\ln\mu}\, a_{\gamma'}(\nu,\mu) &= -\gamma'\big(\alpha_{\rm s}(\mu)\big)\,,
\end{aligned} \tag{12}$$

with initial conditions $S(\nu,\nu) = a_\Gamma(\nu,\nu) = a_{\gamma'}(\nu,\nu) = 0$ at $\mu = \nu$. Here $\Gamma_{\rm cusp}$ is the universal cusp anomalous dimension for Wilson loops with light-like segments [33], which has recently been calculated to three-loop order [34], and $\gamma'$ enters the anomalous dimension of the leading-order SCET current operators containing a heavy quark and a hard-collinear quark with large energy $E$, which takes the form [19, 23]

$$\gamma_J(E,\mu) = -\Gamma_{\rm cusp}\big(\alpha_{\rm s}(\mu)\big)\ln\frac{\mu}{2E} + \gamma'\big(\alpha_{\rm s}(\mu)\big)\,. \tag{13}$$

As explained in Appendix A, a conjecture for the two-loop expression for $\gamma'$ can be deduced using results from the literature on deep-inelastic scattering [35–37]. The evolution equations (12) are solved in the standard way by writing $\mathrm{d}/\mathrm{d}\ln\mu = \beta(\alpha_{\rm s})\,\mathrm{d}/\mathrm{d}\alpha_{\rm s}$, where $\beta(\alpha_{\rm s}) = \mathrm{d}\alpha_{\rm s}/\mathrm{d}\ln\mu$ is the QCD $\beta$ function. This yields the exact solutions

$$\begin{aligned}
S(\nu,\mu) &= -\int\limits_{\alpha_{\rm s}(\nu)}^{\alpha_{\rm s}(\mu)} \mathrm{d}\alpha\, \frac{\Gamma_{\rm cusp}(\alpha)}{\beta(\alpha)} \int\limits_{\alpha_{\rm s}(\nu)}^{\alpha} \frac{\mathrm{d}\alpha'}{\beta(\alpha')}\,, \\
a_\Gamma(\nu,\mu) &= -\int\limits_{\alpha_{\rm s}(\nu)}^{\alpha_{\rm s}(\mu)} \mathrm{d}\alpha\, \frac{\Gamma_{\rm cusp}(\alpha)}{\beta(\alpha)}\,,
\end{aligned} \tag{14}$$

and similarly for the function $a_{\gamma'}$. The perturbative expansions of the anomalous dimensions and the resulting expressions for the evolution functions valid through order $\alpha_{\rm s}$ are collected in Appendix A.

As written in (1), the decay rate is sensitive to non-perturbative hadronic physics via its dependence on the shape function. This sensitivity is unavoidable as long as the scale $\Delta = m_b - 2E_0$ is a hadronic scale, corresponding to the endpoint region of the photon spectrum above, say, 2 GeV. The properties of the $B \to X_s\gamma$ decay rate and photon spectrum in this region will be discussed in detail elsewhere. Here we are interested in a situation where $E_0$ is lowered out of the shape-function region, such that $\Delta$ can be considered large compared with $\Lambda_{\rm QCD}$. For orientation, we note that with $m_b = 4.7\,\mathrm{GeV}$ and the cutoff $E_0 = 1.8\,\mathrm{GeV}$ employed in a recent analysis by the Belle Collaboration [6] one gets $\Delta = 1.1\,\mathrm{GeV}$. For $E_0 = 1.6\,\mathrm{GeV}$ (a reference value adopted in [7, 27], which at present is below what can be achieved experimentally) one would obtain $\Delta = 1.5\,\mathrm{GeV}$. As mentioned in the Introduction, in all previous analyses

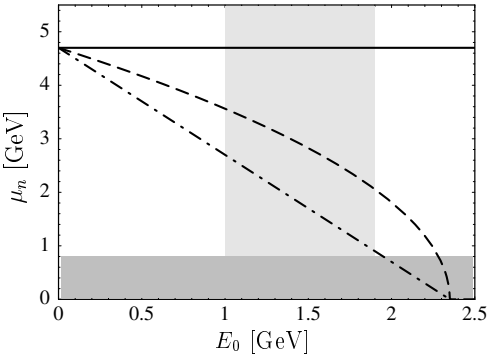


**Fig. 1.** Dependence of the three scales $\mu_h = m_b$ (solid), $\mu_{\rm i} = \sqrt{m_b\Delta}$ (dashed), and $\mu_0 = \Delta$ (dash-dotted) on the cutoff $E_0$, assuming $m_b = 4.7\,\mathrm{GeV}$. The gray area at the bottom shows the domain of non-perturbative physics. The light gray band in the center indicates the region where the MSOPE should be applied

of the $B \to X_s\gamma$ decay rate it was assumed that, once $E_0$ is taken below about 1.9 GeV, the sensitivity to hadronic physics essentially disappears, and the rate can be computed using a conventional OPE at the scale $m_b$. The main point of the present work is to show that this assumption cannot be justified, and that estimating theoretical uncertainties under the hypothesis that the expansion is in powers of $\alpha_{\rm s}(m_b)$ and $\Lambda_{\rm QCD}/m_b$ underestimates the magnitude of the true theoretical errors. As we will show, for values of $E_0$ outside the shape-function region there are three relevant mass scales in the problem besides $\Lambda_{\rm QCD}$. They are the hard scale $m_b$, the hard-collinear scale $\sqrt{m_b\Delta}$, and the low scale $\Delta$ itself. The values of these scales as a function of the photon-energy cutoff $E_0$ are shown in Fig. 1. The transition from the shape-function region to the region where a conventional OPE can be applied is not abrupt but proceeds via an intermediate region, in which a short-distance analysis based on a multi-scale OPE (MSOPE) can be performed. The transition from the shape-function region into the MSOPE region occurs when the scale $\Delta$ becomes numerically (but not parametrically) large compared with $\Lambda_{\rm QCD}$. Then terms of order $\alpha_{\rm s}^n(\Delta)$ and $(\Lambda_{\rm QCD}/\Delta)^n$, which are non-perturbative in the shape-function region, gradually become decent expansion parameters. Only for very low values of the cutoff ($E_0 < 1\,\mathrm{GeV}$ or so) it is justified to treat $\Delta$ and $\sqrt{m_b\Delta}$ as scales of order $m_b$.

Separating the contributions associated with these scales requires a multi-step procedure, which we develop in the present work. The first step, the separation of the hard scale from the intermediate scale, has already been achieved in (1). To proceed further we use two crucial recent developments. First, integrals of smooth weight functions $F(\hat{\omega})$ with the shape function $\hat{S}(\hat{\omega},\mu)$ can be expanded in a series of forward $B$-meson matrix elements of local HQET operators, provided that the integration domain is large compared with $\Lambda_{\rm QCD}$ [14, 15]. The reason is that the shape function can be written as the discontinuity of a two-point correlator in momentum space, and thus weighted integrals over $\hat{S}$ can be turned into contour integrals in the complex plane along a circle with radius set by the upper integra-

tion limit on $\hat\omega$ (more precisely, $\hat\omega - \bar\Lambda$). Specifically, the expansion takes the form [14]

$$\int_0^{\Delta+\bar\Lambda} \mathrm{d}\hat\omega\, \hat S(\hat\omega,\mu)\, F(\hat\omega) = K_0^{(F)}(\Delta,\mu) + K_2^{(F)}(\Delta,\mu)\,\frac{(-\lambda_1)}{3\Delta^2} + \dots\,, \qquad (15)$$

where $K_n^{(F)}$ are calculable Wilson coefficient functions, $\bar\Lambda = m_B - m_b$ and $\lambda_1$ are HQET parameters (which for the time being are defined in the pole scheme) [20], and the dots represent terms of order $(\Lambda_{\rm QCD}/\Delta)^3$ or higher. Note that with $\Delta = m_b - 2E_0$ as defined above we have $\Delta + \bar\Lambda = M_B - 2E_0 = \Delta_E$, which coincides with the upper limit for the integration over $\hat\omega$ in (1). The perturbative expansions of the coefficient functions $K_n^{(F)}$ can be trusted as long as $\mu \sim \Delta$. In order to complete the scale separation, it is therefore necessary to evolve the shape function in (1) from the intermediate scale $\mu_{\rm i} \sim \sqrt{m_b\Delta}$ down to a scale $\mu_0 \sim \Delta$. This can be achieved using the analytic solution to the integro-differential RG evolution equation for the shape function in momentum space obtained in [14, 18]. These manipulations will be discussed in detail in the following two sections.

As a final comment, we stress that the main purpose of performing the scale separation using the MSOPE is not that this allows us to resum Sudakov logarithms by solving RG equations. Indeed, the "large logarithm" $\ln(m_b/\Delta) \approx 1.5$ is only parametrically large, but not numerically. What is really important is to disentangle the physics at the low scale $\mu_0 \sim \Delta$, which is "barely perturbative", from the physics associated with higher scales, where a short-distance treatment is on much safer grounds. It would be wrong to pretend that all perturbative effects in $B \to X_s\gamma$ decays are associated with the short-distance scale $m_b \gg \Lambda_{\rm QCD}$. The MSOPE allows us to distinguish between the three coupling constants $\alpha_{\rm s}(m_b) \approx 0.22$, $\alpha_{\rm s}(\sqrt{m_b\Delta}) \approx 0.29$, and $\alpha_{\rm s}(\Delta) \approx 0.44$ (for $\Delta = 1.1\,\mathrm{GeV}$), which are rather different despite the fact that there are no numerically large logarithms in the problem. Given the values of these couplings, we expect that scale separation between $\Delta$ and $m_b$ is as important as that between $m_b$ and the weak scale $M_W$.

## 3 Evolution of the shape function

The renormalized shape function obeys the integro-differential RG evolution equation

$$\frac{\mathrm{d}}{\mathrm{d}\ln\mu}\,\hat S(\hat\omega,\mu) = -\int \mathrm{d}\hat\omega'\,\gamma_S(\hat\omega,\hat\omega',\mu)\,\hat S(\hat\omega',\mu)\,, \qquad (16)$$

where the anomalous dimension can be written in the form

$$\gamma_S(\hat\omega,\hat\omega',\mu) = -2\Gamma_{\rm cusp}\big(\alpha_{\rm s}(\mu)\big)\left[\frac{1}{\hat\omega-\hat\omega'}\right]_*^{[\mu]} + 2\gamma\big(\alpha_{\rm s}(\mu)\big)\,\delta(\hat\omega-\hat\omega')\,. \qquad (17)$$

This form was found in two recent one-loop calculations of the ultra-violet poles of non-local HQET operators [14,15]. A brief history of previous investigations of the anomalous-dimension kernel can be found in the first reference. The structure of (17) was derived first by Grozin and Korchemsky [38], who also computed the anomalous dimension and argued that the functional form of $\gamma_S(\hat\omega,\hat\omega',\mu)$ shown above holds to all orders in perturbation theory. A conjecture for the two-loop expression of the anomalous dimension $\gamma$ is presented in Appendix A.

The exact solution to (16) can be found using a technique developed in [18]. The equation is solved by the remarkably simple form

$$\hat S(\hat\omega,\mu_{\rm i}) = U_2(\mu_{\rm i},\mu_0)\,\frac{\mathrm{e}^{-\gamma_{\rm E}\eta}}{\Gamma(\eta)}\int_0^{\hat\omega}\mathrm{d}\hat\omega'\,\frac{\hat S(\hat\omega',\mu_0)}{\mu_0^\eta(\hat\omega-\hat\omega')^{1-\eta}}\,, \qquad (18)$$

where

$$\ln U_2(\mu_{\rm i},\mu_0) = 2S(\mu_0,\mu_{\rm i}) + 2a_\gamma(\mu_0,\mu_{\rm i})\,, \qquad \eta = -2a_\Gamma(\mu_0,\mu_{\rm i})\,. \qquad (19)$$

The functions $S$ and $a_\Gamma$ have been defined in (12). Similarly, the function $a_\gamma$ is defined in complete analogy with $a_{\gamma'}$, but with $\gamma'$ replaced with the anomalous dimension $\gamma$ in (17). Explicit equations for these functions are given in Appendix A. The next-to-leading logarithmic approximation to (18) was first derived in [14]. We note that a similar (but not identical) result was found in [39] based on a one-loop calculation of the anomalous-dimension kernel.

Relation (18) accomplishes the evolution of the shape function from the intermediate scale down to the low scale $\mu_0 \sim \Delta$. When this result is inserted into the factorization formula (1), it is possible to perform the integrations over $P_+$ and $\hat\omega$ analytically, leaving the integration over $\hat\omega'$ until the end. Using the expression for the jet function in (9), we find that the leading contribution to the decay rate is given by

$$\Gamma^{\rm leading}_{\bar B\to X_s\gamma}(E_0) = \frac{G_{\rm F}^2\alpha}{32\pi^4}\,|V_{tb}V_{ts}^*|^2\,(1+\varepsilon_{\rm np})\,\overline{m}_b^2(\mu_h)\,|H_\gamma(\mu_h)|^2 \times U_1(\mu_h,\mu_{\rm i})\,U_2(\mu_{\rm i},\mu_0)\,\frac{\mathrm{e}^{-\gamma_{\rm E}\eta}}{\Gamma(1+\eta)}\,I(E_0)\,, \qquad (20)$$

where

$$I(E_0) = \int_0^{\Delta_E}\mathrm{d}\hat\omega\,\hat S(\hat\omega,\mu_0)\,(M_B-\hat\omega)^3\left(\frac{\Delta_E-\hat\omega}{\mu_0}\right)^\eta \times\left[1+\frac{C_F\alpha_{\rm s}(\mu_{\rm i})}{4\pi}\,\mathcal{J}(\Delta_E-\hat\omega)\right]p_3\left(\eta,\frac{\Delta_E-\hat\omega}{M_B-\hat\omega}\right). \qquad (21)$$

The function $p_3(\eta,\delta)$ is a special case of the polynomial

$$p_n(\eta,\delta) = \sum_{k=0}^n\binom{n}{k}\frac{\eta\,(-\delta)^k}{k+\eta} \quad\Rightarrow\quad p_3(\eta,\delta) = 1 - \frac{3\eta\delta}{1+\eta} + \frac{3\eta\delta^2}{2+\eta} - \frac{\eta\delta^3}{3+\eta}\,. \qquad (22)$$

The next-to-leading order corrections from the jet function are encoded in the operator

$$\mathcal{J}(\Delta) = 2\left(\ln\frac{m_b\Delta}{\mu_{\rm i}^2} + \partial_\eta\right)^2 - \big[4h(\eta)+3\big]\left(\ln\frac{m_b\Delta}{\mu_{\rm i}^2} + \partial_\eta\right) + 2h^2(\eta) + 3h(\eta) - 2h'(\eta) + 7 - \frac{2\pi^2}{3}\,, \tag{23}$$

where

$$h(\eta) = \psi(\eta) + \gamma_{\rm E} + \frac{1}{\eta} = \psi(1+\eta) + \gamma_{\rm E} \tag{24}$$

is the harmonic function generalized to non-integer argument, and the derivatives $\partial_\eta = \partial/\partial\eta$ in (23) act on the function $p_3(\eta,\delta)$ in (21). Note that this result has a smooth limit for $\mu_0 \to \mu_{\rm i}$, in which case $\eta \to 0$, $U_2(\mu_{\rm i},\mu_0) \to 1$, $h(\eta) \to 0$, $h'(\eta) \to \pi^2/6$, and we obtain an expression equivalent to the original result in (1).

## 4 Short-distance expansion of the convolution integral

The remaining task is to expand the integral over the shape function in (21) using an OPE, relating it to forward $B$-meson matrix elements of local HQET operators, as indicated in (15). As explained in [14], this can be done whenever $\Delta = \Delta_E - \bar\Lambda = m_b - 2E_0$ is large compared with $\Lambda_{\rm QCD}$. For a given weight function $F$, the matching coefficients $K_n^{(F)}$ are determined in the usual way by computing the integral in perturbation theory, expanding in powers of external momenta, and writing the answer as a linear combination of Wilson coefficients multiplying the matrix elements of local HQET operators. This matching calculation can be done using free partons in the external states and employing any infra-red regulator scheme that is convenient. We use on-shell external heavy-quark states with residual momentum $k$ chosen such that $v\cdot k = 0$. In this case, the perturbative expression for the renormalized shape function at one-loop order is [14, 15]

$$\hat S_{\rm parton}(\hat\omega,\mu_0) = \delta(\hat\omega - \bar\Lambda + n\cdot k)\left(1 - \frac{C_F\alpha_{\rm s}(\mu_0)}{\pi}\,\frac{\pi^2}{24}\right) - \frac{C_F\alpha_{\rm s}(\mu_0)}{\pi} \times \left[\frac{1}{\hat\omega - \bar\Lambda + n\cdot k}\left(2\ln\frac{\hat\omega - \bar\Lambda + n\cdot k}{\mu_0} + 1\right)\right]_*^{[\mu_0]}. \tag{25}$$

Using this result one can perform the integral over the shape function in (21) analytically. The answer is then Taylor-expanded in powers of $n\cdot k$. The terms up to second order in this expansion are identified with the forward $B$-meson matrix elements of the operators $\bar h h$, $\bar h\, in\cdot D h$, and $\bar h\,(in\cdot D)^2 h$, respectively, where $n^\mu = (1,0,0,1)$ is a light-like vector. The values of these matrix elements are given by 1, 0, and $-\lambda_1/3$ [8]. They do not receive radiative corrections in the regularization scheme adopted here. Operators of dimension six or higher would mix under renormalization. Also, in order to find their Wilson coefficients it would be necessary to perform matching calculations with external gluon states. However, it will be sufficient for all practical purposes to truncate the expansion after the second term, keeping only operators of dimension up to five. The result of this calculation is

$$I(E_0) = m_b^3\left(\frac{\Delta}{\mu_0}\right)^\eta \times \left[1 + \frac{C_F\alpha_{\rm s}(\mu_{\rm i})}{4\pi}\,\mathcal{J}(\Delta) + \frac{C_F\alpha_{\rm s}(\mu_0)}{4\pi}\,\mathcal{S}(\Delta)\right] \times \left[p_3\left(\eta,\frac{\Delta}{m_b}\right) + \frac{\eta(\eta-1)}{2}\,\frac{(-\lambda_1)}{3\Delta^2} + \ldots\right], \tag{26}$$

where $\mathcal{J}(\Delta)$ has been defined in (23), and

$$\mathcal{S}(\Delta) = -4\left(\ln\frac{\Delta}{\mu_0} + \partial_\eta\right)^2 + 4\,[2h(\eta)-1]\left(\ln\frac{\Delta}{\mu_0} + \partial_\eta\right) - 4h^2(\eta) + 4h(\eta) + 4h'(\eta) - \frac{5\pi^2}{6}\,. \tag{27}$$

We have restricted ourselves to include only the leading power correction of order $\lambda_1/\Delta^2$, dropping terms that are suppressed by additional powers of $\Delta/m_b$. This is necessary for consistency, because there exist other, unknown $1/m_b$ and $1/m_b^2$ corrections from subleading shape functions, i.e., non-local HQET operators containing additional derivatives or insertions of soft gluon fields [40]. The $\lambda_1/\Delta^2$ term is obtained by acting with $(-\lambda_1/6)\,\partial_\Delta^2$ on the leading-order term. According to (26), its effect can be included by simply adding a power correction to the function $p_3(\eta,\delta)$.

The reader may ask why such an "enhanced" power correction was not found in previous analyses of the decay $B \to X_s\gamma$, or of the related semileptonic decay $B \to X_u\, l\,\nu$. Common lore is that non-perturbative corrections to inclusive decay rates scale like $(\Lambda_{\rm QCD}/m_b)^2$ and thus are very small. The reason is that so far power corrections in the OPE were computed at tree level only (an exception being [41]). While the terms displayed above have a non-zero leading-order coefficient after RG resummation, they vanish at tree level if the result is expanded in fixed-order perturbation theory. Explicitly, we find to first order in $\alpha_{\rm s}$

$$\frac{I(E_0)}{m_b^3} \ni \frac{(-\lambda_1)}{3\Delta^2}\,\frac{C_F\alpha_{\rm s}}{4\pi}\left(-2\ln\frac{m_b}{\Delta} + \frac{3}{2}\right). \tag{28}$$

This effect would have shown up in the conventional heavy-quark expansion, if power corrections had been computed beyond the tree approximation.

Even though it is parametrically larger than the non-perturbative corrections from the conventional OPE in (2), the enhanced power correction in (26) remains small for

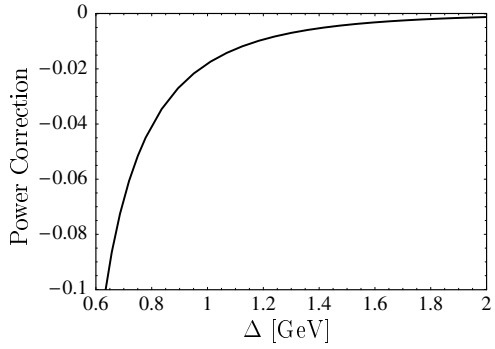


**Fig. 2.** Size of the enhanced power correction proportional to $\lambda_1/\Delta^2$ in (26) relative to the leading term, as a function of $\Delta = m_b - 2E_0$

all relevant values of $\Delta$. This is illustrated in Fig. 2, which shows the size of the power correction proportional to $\lambda_1$ to the function $I(E_0)$ relative to the leading-order term. In the region of "perturbative" values of $\Delta$, where the MSOPE can be trusted, the effect amounts to a reduction of the decay rate by less than 5%. It also follows that subleading power corrections of order $\lambda_1/(m_b\Delta)$ can safely be neglected.

Equation (26), combined with (20), is our main result. Its numerical implications will be analyzed later, after including additional, small power-suppressed terms. A few comments are in order already at this point.

1. The rate in (20) is formally independent of the three matching scales, at which we switch from QCD to SCET ($\mu_h$), from SCET to HQET ($\mu_i$), and finally at which the non-local HQET matrix element (the shape-function integral) is expanded in a series of local operators ($\mu_0$). The explicit perturbative expressions for the functions $H_\gamma(\mu_h)$ in (4), $\mathcal{J}(\Delta)$ in (23), and $\mathcal{S}(\Delta)$ in (27) suggest that the "natural" choices for the three scales are $\mu_h = m_b$, $\mu_i = \sqrt{m_b\Delta}$, and $\mu_0 = \Delta$, as this removes all logarithms from these expressions. The latter two assignments are supported by the observation that, for a typical value $\eta \approx 0.25$, the coefficient function $\mathcal{J}(\Delta)$ vanishes near $\mu_i = 1.08\sqrt{m_b\Delta}$, while $|\mathcal{S}(\Delta)|$ is minimized near $\mu_0 = 1.16\Delta$. Below, we will adopt the "natural" choices as our default values. In practice, a residual scale dependence arises because of the truncation of the perturbative expansion. Varying the three matching scales about their default values provides some information about unknown higher-order perturbative terms .

2. In the limit where the intermediate and low matching scales $\mu_i$ and $\mu_0$ are set equal to the hard matching scale $\mu_h$, our result reduces to the conventional formula used in previous analyses of the $B \to X_s\gamma$ decay rate. However, this choice cannot be justified on physical grounds .

3. After RG resummation the decay rate has a non-trivial dependence on the photon-energy cut $E_0$ already at leading order in RG-improved perturbation theory and at leading power in $\Delta/m_b$, as reflected by the appearance of $\Delta^\eta$ in (26). Apart from small logarithmic corrections encoded in the functions $\mathcal{J}$ and $\mathcal{S}$, it follows that for $m_b - 2E_\gamma \gg \Lambda_{\rm QCD}$ the photon spectrum exhibits a radiation tail, $\mathrm{d}\Gamma/\mathrm{d}E_\gamma \propto 1/(m_b - 2E_\gamma)^{1-\eta}$, which has a slow fall-off with energy .

4. In (20) we have accomplished a complete resummation of (parametrically) large logarithms at next-to-next-to-leading logarithmic order in RG-improved perturbation theory, which is necessary in order to calculate the decay rate with $\mathcal{O}(\alpha_s)$ accuracy. This is highly non-trivial in cases where Sudakov double logarithms are present. Specifically, it means that terms of the form $\alpha_s^n L^k$ with $k = (n-1), \ldots, 2n$ and $L = \ln(m_b/\Delta)$ are correctly resummed to all orders in perturbation theory. At a given order $\alpha_s^n$, there are $(n+2)$ such terms. To the best of our knowledge, a complete resummation at next-to-next-to-leading order has never been achieved before. For ease of comparison with the results of other authors, we provide in Appendix B an expansion of our result to second order in $\alpha_s$, deriving the coefficients of the terms $\alpha_s^2 L^k$ with $k = 1, 2, 3, 4$ .

5. Finally, we stress that the various next-to-leading order corrections in the expression for the decay rate obtained from (20) and (26) should be consistently expanded to order $\alpha_s$ before applying our results to phenomenology. Such next-to-leading order terms are contained in the functions $C_{7\gamma}^{\rm eff}(\mu_h)$, $\overline{m}_b(\mu_h)$, $H_\gamma(\mu_h)$, $U_1(\mu_h,\mu_i)$, $U_2(\mu_i,\mu_0)$, $\eta$, and $I(E_0)$. For instance, one should expand

$$\frac{\mathrm{e}^{-\gamma_E\eta}}{\Gamma(1+\eta)} = \frac{\mathrm{e}^{-\gamma_E\eta_0}}{\Gamma(1+\eta_0)} \times \left[1 - \frac{\Gamma_0}{\beta_0}\left(\frac{\Gamma_1}{\Gamma_0} - \frac{\beta_1}{\beta_0}\right)\frac{\alpha_s(\mu_0) - \alpha_s(\mu_i)}{4\pi}\,h(\eta_0) + \ldots\right], \tag{29}$$

where $\eta_0 = \frac{\Gamma_0}{\beta_0}\ln\frac{\alpha_s(\mu_0)}{\alpha_s(\mu_i)}$ is the leading-order expression for $\eta$ (see Appendix A). In practice, these expansions are readily automatized.

## 5 Elimination of pole-scheme parameters

The expression for the function $I(E_0)$ in (26) has been derived under the implicit assumption that the $b$-quark mass $m_b$, the related parameter $\Delta = m_b - 2E_0$, and the HQET parameter $\lambda_1$ are defined in the on-shell scheme. While this is most convenient for performing calculations using heavy-quark expansions, it is well known that HQET parameters defined in the pole scheme suffer from infra-red renormalon ambiguities [42–45]. As a result, the perturbative expansion in (26) would not be well behaved. It is thus necessary to replace the pole mass $m_b$ and the HQET parameter $\lambda_1$ in favor of some physical, short-distance parameters.

For our purposes, the "shape-function scheme" defined in [14] provides for a particularly suitable definition of the heavy-quark mass and kinetic energy. A look at (21) shows that the pole mass actually never enters the expression for the decay rate. Rather, a factor $(M_B - \hat{\omega})^3$ appears under the integral over the shape function, which can be traced back to the factor $(M_B - P_+)^3 = 8E_\gamma^3$ in the original expression for the rate in (1). Roughly speaking, it is the average value of $\hat{\omega}$ that determines the value of the difference $(M_B - \hat{\omega})$. This observation is the basis of the shape-function scheme. The idea is that a good estimate of the right-hand side of (21) can be obtained using the mean-value theorem, i.e., by replacing $\hat{\omega}$ with its mean

value defined as

$$\langle\hat\omega\rangle_\Delta = \frac{\int_0^{\Delta_E} d\hat\omega\,\hat\omega\,\hat S(\hat\omega,\mu_0)}{\int_0^{\Delta_E} d\hat\omega\,\hat S(\hat\omega,\mu_0)} \equiv \bar\Lambda(\Delta,\mu_0) = M_B - m_b(\Delta,\mu_0)\,. \tag{30}$$

Here $m_b(\Delta,\mu_0)$ is the running shape-function mass defined in [14], which depends on a hard cutoff $\Delta$ in addition to the renormalization scale $\mu_0$. The quantity $\Delta$ in the shape-function scheme is defined by the implicit equation

$$\Delta = \Delta_E - \bar\Lambda(\Delta,\mu_0) = m_b(\Delta,\mu_0) - 2E_0\,. \tag{31}$$

(For simplicity, we write $\Delta$ instead of the more correct notation $\Delta(\Delta,\mu_0)$.) Likewise, we define a kinetic-energy parameter $\mu_\pi^2(\Delta,\mu_0)$ via the variance of $\hat\omega$,

$$\langle\hat\omega^2\rangle_\Delta - \langle\hat\omega\rangle_\Delta^2 = \frac{\int_0^{\Delta_E} d\hat\omega\,\hat\omega^2\,\hat S(\hat\omega,\mu_0)}{\int_0^{\Delta_E} d\hat\omega\,\hat S(\hat\omega,\mu_0)} - \langle\hat\omega\rangle_\Delta^2 \equiv \frac{\mu_\pi^2(\Delta,\mu_0)}{3}\,. \tag{32}$$

The shape-function scheme provides a physical, short-distance definition of $m_b$ and $\mu_\pi^2$, which can be related to any other short-distance definition of these parameters using perturbation theory. The explicit form of these relations for some common renormalization schemes can be found in [14]. Here we need the relations to the parameters defined in the pole scheme. They are

$$\begin{aligned} m_b^{\rm pole} &= m_b(\Delta,\mu_0) \\ &\quad + \Delta\,\frac{C_F\alpha_s(\mu_0)}{\pi} \\ &\quad \times\left[\left(1 - 2\ln\frac{\Delta}{\mu_0}\right) + \frac{2}{3}\,\frac{\mu_\pi^2(\Delta,\mu_0)}{\Delta^2}\,\ln\frac{\Delta}{\mu_0}\right] + \dots\,, \\ -\lambda_1 &= \mu_\pi^2(\Delta,\mu_0)\left[1 + \frac{C_F\alpha_s(\mu_0)}{\pi}\left(-3\ln\frac{\Delta}{\mu_0} - \frac{1}{2}\right)\right] \\ &\quad + 3\Delta^2\,\frac{C_F\alpha_s(\mu_0)}{\pi}\,\ln\frac{\Delta}{\mu_0} + \dots \end{aligned} \tag{33}$$

The corresponding relation for $\Delta^{\rm pole}$ follows from the fact that $\Delta^{\rm pole} = m_b^{\rm pole} - 2E_0$. In order to introduce the parameters defined in the shape-function scheme, we perform these replacements in the expression for $I(E_0)$ in (26) and expand the result consistently to order $\alpha_s$. (In the next-to-leading order terms we can simply replace the parameters of the pole scheme by the corresponding parameters of the shape-function scheme.)

While the above choice appears most natural to us, it is by no means unique. For instance, we may avoid using the running quantities $m_b(\mu_f,\mu)$ and $\mu_\pi^2(\mu_f,\mu)$ with "off-diagonal" scale choices $\mu_f \neq \mu$ by using instead the parameters $m_b(\mu,\mu)$ and $\mu_\pi^2(\mu,\mu)$, which are related to the parameters in the pole scheme by the simpler relations

$$\begin{aligned} m_b^{\rm pole} &= m_b(\mu,\mu) + \mu\,\frac{C_F\alpha_s(\mu)}{\pi} + \dots\,, \\ -\lambda_1 &= \mu_\pi^2(\mu,\mu)\left[1 - \frac{C_F\alpha_s(\mu)}{2\pi}\right] + \dots \end{aligned} \tag{34}$$

The parameter $\Delta$ is now determined by the equation $\Delta = m_b(\mu,\mu) - 2E_0$. The scale $\mu$ could naturally be taken to be $\mu_0$. Alternatively, we may use the parameters of the shape-function scheme defined at a fixed reference scale $\mu_* = 1.5\,\text{GeV}$, at which their values have been determined to be $m_b(\mu_*,\mu_*) = (4.65 \pm 0.07)\,\text{GeV}$ and $\mu_\pi^2(\mu_*,\mu_*) = (0.27 \pm 0.07)\,\text{GeV}^2$ [14]. These determinations are based on various sources of phenomenological information, including $\Upsilon$ spectroscopy and moments of inclusive $B$-meson decay spectra. In our numerical analysis in Sect. 8 we will present results for different variants of the shape-function scheme.

## 6 Kinematic power corrections

The results of the previous section provide a complete description of the $B \to X_s\gamma$ decay rate at leading order in the $1/m_b$ expansion, where the two-step matching procedure QCD $\to$ SCET $\to$ HQET is well understood. The matching coefficients and anomalous dimensions are known to the required order, so that the scale separation and RG resummation can be carried out with next-to-next-to-leading logarithmic accuracy. For practical applications, however, it is necessary to also include corrections arising at higher orders in the heavy-quark expansion. The leading non-perturbative corrections proportional to the HQET parameter $\lambda_1$ (or $\mu_\pi^2$) have already been included above. More important, however, are "kinematic" power corrections of order $(\Delta/m_b)^n$, which are not associated with new hadronic parameters. Unlike the non-perturbative corrections, these effects arise already at first order in $\Delta/m_b$, and they are numerically dominant in the region where $\Delta \gg \Lambda_{\rm QCD}$. Technically, the kinematic power corrections arise in the matching of QCD correlators onto higher-dimensional SCET and HQET operators.

The corresponding terms are known in fixed-order perturbation theory, without scale separation and RG resummation [26, 46] (see also [17]). To perform a complete RG analysis of even the first-order terms in $\Delta/m_b$ is beyond the scope of the present work. Since for typical values of $E_0$ the power corrections only account for about 15% of the $B \to X_s\gamma$ decay rate, an approximate treatment will suffice. To motivate it, we note the following two facts: First, while the anomalous dimensions of the relevant subleading SCET and HQET operators are only known for a few cases [47], the leading Sudakov double logarithms are determined by the cusp anomalous dimension and thus are the same as for the terms of leading power. The reason is that the cusp anomalous dimension has a geometric origin. In the present case, it results from a product of time-like and light-like Wilson lines describing heavy and hard-collinear quark fields, respectively [48]. The leading Sudakov double logarithms are therefore the same as those

resummed into the exponents $S(\mu_h,\mu_{\rm i})$ and $S(\mu_0,\mu_{\rm i})$ contained in the evolution functions $U_1$ and $U_2$ in (11) and (19). Secondly, all power-suppressed terms of order $(\Delta/m_b)^n$ are associated with gluon emission into the hadronic final state $X_s$. Because of the kinematic restriction to low-mass final states, i.e. $M_X^2 \le M_B\Delta_E$, the emitted gluon can only be hard-collinear or soft, but not hard. One should therefore associate a coupling $\alpha_{\rm s}(\mu_{\rm i})$ or $\alpha_{\rm s}(\mu_0)$ with these terms. The leading power corrections are then of order $\alpha_{\rm s}(\mu)\,\delta\ln\delta$ with $\delta=\Delta/m_b$ and $\mu\sim\mu_{\rm i}$ or $\mu_0$. After RG resummation, they can give rise to effects of order $\eta\,\delta$, which are formally of zeroth order in the coupling constant. Not resolving the scale ambiguity for such terms introduces an uncertainty that is at most of order $\alpha_{\rm s}^2\ln^2\delta$.

In order to at least partially account for resummation effects, we proceed as follows: We include the known power corrections from real gluon emission and associate the coupling $\alpha_{\rm s}(\mu_{\rm i})$ with them. The Wilson coefficients $C_i$ are evaluated at the hard scale $\mu_h$. We then multiply the answer with the evolution function $U_1$. This accounts correctly for the leading Sudakov logarithms in the evolution from the hard scale $\mu_h$ to the intermediate scale $\mu_{\rm i}$. While the conventional parton-model calculation of the $B\to X_s\gamma$ decay rate is performed with on-shell $b$ quarks, we add a residual momentum such that $p_b = m_b v + k$. In the light-cone component $n\cdot p_b = m_b + n\cdot k$ we keep the $n\cdot k$ piece, because it is of the same order as the corresponding component $n\cdot p_{hc}$ of a hard-collinear momentum. In all other components we neglect $k$. This accounts for some, but not all shape-function effects. The net result is that we must replace $m_b\to M_B-\hat\omega$ (and hence $\Delta_E\to\Delta_E-\hat\omega$) in the parton-model calculation, and then convolute the result with the leading-order shape function. In the approximation where the small parameter $\varepsilon_{\rm CKM}$ in (5) is set to zero (which is an excellent approximation given that we are dealing with power-suppressed effects), this yields

$$\begin{aligned}
&\Gamma^{\rm power}_{\bar B\to X_s\gamma}(E_0)\\
&= \frac{G_{\rm F}^2\alpha}{32\pi^4}\,|V_{tb}V_{ts}^*|^2\,\overline{m}_b^2(\mu_h)\,U_1(\mu_h,\mu_{\rm i})\\
&\quad\times\int_0^{\Delta_E}\!{\rm d}\hat\omega\,\hat S(\hat\omega,\mu_{\rm i})\,(M_B-\hat\omega)^3\\
&\quad\times\Bigg[\frac{C_F\alpha_{\rm s}(\mu_{\rm i})}{4\pi}\sum_{\substack{i,j=1,7,8\\ i\le j}}{\rm Re}\Big(C_i^*(\mu_h)\,C_j(\mu_h)\Big)\\
&\qquad\qquad\times\hat f_{ij}\left(\frac{\Delta_E-\hat\omega}{M_B-\hat\omega}\right)\\
&\qquad-{\rm Re}\Big(C_1^*(\mu_h)\,C_{7\gamma}^{\rm eff}(\mu_h)\Big)\,\frac{\lambda_2}{9m_c^2}\Bigg]\,. \qquad (35)
\end{aligned}$$

The functions $\hat f_{ij}(\delta)$ vanish linearly with $\delta$ and so are of order $\Delta/m_b$. They coincide with $3f_{ij}(\delta)$ in [17] except for the case of $\hat f_{77}(\delta)$, which requires an additional subtraction due to the fact that the function $p_3(\eta,\delta)$ in (26) already contains some power corrections resulting from the presence of the factor $(M_B-P_+)^3$ in (1). We find

$$\begin{aligned}
\hat f_{77}(\delta) &= 3f_{77}(\delta) - \delta\,(12\ln\delta+9) + \delta^2\left(6\ln\delta+\frac{15}{2}\right)\\
&\quad-\delta^3\left(\frac{4}{3}\ln\delta+\frac{17}{9}\right). \qquad (36)
\end{aligned}$$

The relevant expressions are

$$\begin{aligned}
\hat f_{77}(\delta) &= \delta+\frac{17\delta^2}{2}-\frac{23\delta^3}{9}-\delta\left(16-7\delta+\frac{4\delta^2}{3}\right)\ln\delta\,,\\
\hat f_{88}(\delta) &= \frac{4}{9}\,\Bigg\{L_2(1-\delta)-\frac{\pi^2}{6}+2\ln(1-\delta)\\
&\quad-\frac{\delta}{4}\,(2+\delta)\ln\delta+\frac{7\delta}{4}+\frac{3\delta^2}{4}-\frac{\delta^3}{6}\\
&\quad-\left[\delta+\frac{\delta^2}{2}+2\ln(1-\delta)\right]\ln\frac{m_b}{m_s}\Bigg\}\,,\\
\hat f_{78}(\delta) &= \frac{8}{3}\left[L_2(1-\delta)-\frac{\pi^2}{6}-\delta\ln\delta+\frac{9\delta}{4}-\frac{\delta^2}{4}+\frac{\delta^3}{12}\right],\\
\hat f_{11}(\delta) &= \frac{16}{9}\int_0^1{\rm d}x\,(1-x)(1-x_\delta)\,\left|\,\frac{z}{x}\,G\Big(\frac{x}{z}\Big)+\frac{1}{2}\,\right|^2,\\
\hat f_{17}(\delta) &= -3\hat f_{18}(\delta)\\
&= -\frac{8}{3}\int_0^1{\rm d}x\,x(1-x_\delta)\,{\rm Re}\left[\,\frac{z}{x}\,G\Big(\frac{x}{z}\Big)+\frac{1}{2}\,\right], \qquad (37)
\end{aligned}$$

where $x_\delta=\max(x,1-\delta)$, as previously $z=(m_c/m_b)^2$, and

$$G(t)=\begin{cases}-2\arctan^2\sqrt{t/(4-t)} & ;\ t<4\,,\\ 2\left(\ln\Big[(\sqrt{t}+\sqrt{t-4})/2\Big]-\dfrac{{\rm i}\pi}{2}\right)^2 & ;\ t\ge4\,.\end{cases} \qquad (38)$$

The next step is to account for the evolution between $\mu_{\rm i}$ and $\mu_0$, and to evaluate the shape-function integrals for $\Delta\gg\Lambda_{\rm QCD}$ using the techniques described in Sect. 4. From (18) and (25), we find

$$\hat S_{\rm parton}(\hat\omega,\mu_{\rm i}) = U_2(\mu_{\rm i},\mu_0)\,\frac{{\rm e}^{-\gamma_{\rm E}\eta}}{\Gamma(\eta)}\,\frac{\theta(\hat\omega-\bar\Lambda)}{\mu_0^\eta(\hat\omega-\bar\Lambda)^{1-\eta}}+\ldots\,, \qquad (39)$$

where $\bar\Lambda$ is defined in the shape-function scheme (see Sect. 5), and the dots represent terms of order $\alpha_{\rm s}(\mu_0)$ and higher-order non-perturbative corrections, which we consistently neglect. Inserting this result into (35) yields

$$\begin{aligned}
&\Gamma^{\rm power}_{\bar B\to X_s\gamma}(E_0) = \frac{G_{\rm F}^2\alpha}{32\pi^4}\,|V_{tb}V_{ts}^*|^2\,\overline{m}_b^2(\mu_h)\\
&\times U_1(\mu_h,\mu_{\rm i})\,U_2(\mu_{\rm i},\mu_0)\,\frac{{\rm e}^{-\gamma_{\rm E}\eta}}{\Gamma(1+\eta)}\,m_b^3\left(\frac{\Delta}{\mu_0}\right)^\eta p_3\left(\eta,\frac{\Delta}{m_b}\right)\\
&\times\Bigg[\frac{C_F\alpha_{\rm s}(\mu_{\rm i})}{4\pi}\sum_{\substack{i,j=1,7,8\\ i\le j}}{\rm Re}\Big(C_i^*(\mu_h)\,C_j(\mu_h)\Big)F_{ij}
\end{aligned}$$

$$\times \left(\eta, \frac{\Delta}{m_b}\right) - \mathrm{Re}\left(C_1^*(\mu_h)\, C_{7\gamma}^{\rm eff}(\mu_h)\right) \frac{\lambda_2}{9m_c^2}\Bigg], \tag{40}$$

where

$$F_{ij}(\eta,\delta) = \frac{1}{p_3(\eta,\delta)} \int_0^1 \mathrm{d}y\, \eta\, y^{\eta-1}(1-y\delta)^3\, \hat{f}_{ij}\left(\frac{(1-y)\delta}{1-y\delta}\right). \tag{41}$$

The definition of the "smeared" functions $F_{ij}(\eta,\delta)$ is such that $F_{ij}(0,\delta) = \hat{f}_{ij}(\delta)$, $F_{ij}(\eta,0) = \hat{f}_{ij}(0) = 0$, and $F_{ij}(\eta,1) = \hat{f}_{ij}(1)$.

The result (40) has the desired features that the leading Sudakov double logarithms are correctly resummed in the product $U_1\, U_2$, and that the gluon-emission terms are associated with a low-scale coupling constant that is larger than $\alpha_{\rm s}(\mu_h)$. However, we stress that while the result is correct when expanded in fixed-order perturbation theory to first order in $\alpha_{\rm s}$, the resummation of single logarithmic terms is only approximate. After a complete RG resummation, terms of the form $\alpha_{\rm s}\ln(\Delta/m_b)$, which arise from the $\ln\delta$ terms in the expressions for the functions $\hat{f}_{ij}$, would be resummed into functions of $\eta$, e.g.

$$\frac{C_F\alpha_{\rm s}(\mu_{\rm i})}{\pi}\ln\frac{m_b}{\Delta} \to \eta + \frac{C_F\alpha_{\rm s}(\mu_{\rm i})}{\pi}\ln\frac{m_b\Delta}{\mu_{\rm i}^2} - \frac{2C_F\alpha_{\rm s}(\mu_0)}{\pi}\ln\frac{\Delta}{\mu_0} + \dots \tag{42}$$

The correct answer will contain more complicated functions of $\eta$ as well as non-logarithmic next-to-leading-order corrections at the scales $\mu_{\rm i}$ and $\mu_0$.

While we expect that (40) gives a good approximation for the power-suppressed contributions to the $B \to X_s\gamma$ decay rate, it would be important and conceptually interesting to explore the structure of power corrections further, using the effective field-theory technology developed here and in [14]. It should be possible (with a significant amount of work) to resolve the scale ambiguity for the first-order power corrections in $\Delta/m_b$. Also, an effective field-theory analysis would allow a more rigorous description of certain non-perturbative effects, such as the $\lambda_2/m_c^2$ term in (35), which models a long-distance contribution related to charm-penguin diagrams [49,50], or the logarithmic mass singularity regularized by $m_s$ in the expression for $\hat{f}_{88}$ in (37), which is related to fragmentation effects [51]. More generally, such an analysis would provide a transparent power counting for any long-distance contributions involving soft partons (not only heavy quarks) in the MSOPE.

## 7 Ratios of decay rates

The contributions from the three different short-distance scales entering our central result (20) and the associated theoretical uncertainties can be disentangled by taking ratios of decay rates. Some ratios probe truly short-distance physics (i.e., physics above the scale $\mu_h \sim m_b$) and so remain unaffected by the new theoretical results obtained in this paper. For some other ratios, the short-distance physics associated with the hard scale cancels to a large extent, so that one probes physics at the intermediate and low scales, irrespective of the short-distance structure of the theory. These ratios are important, because they are insensitive to new physics and just probe the interplay of hard-collinear and low scales in the process. Below, we investigate examples of both classes of ratios.

### 7.1 Ratios insensitive to low-scale physics

Most importantly, physics beyond the standard model may affect the theoretical results for the $B \to X_s\gamma$ branching ratio and $CP$ asymmetry only via the Wilson coefficients of the various operators in the effective weak Hamiltonian. (An exception are unconventional new physics scenarios with new light particles, such as a supersymmetric model with light gluinos and $\tilde{b}$ squarks considered in [52].) As a result, the ratio of the $B \to X_s\gamma$ decay rate in a new physics model relative to that in the standard model remains largely unaffected by the resummation effects studied in the present work. From (20), we obtain

$$\frac{\Gamma_{\bar{B}\to X_s\gamma}|_{\rm NP}}{\Gamma_{\bar{B}\to X_s\gamma}|_{\rm SM}} = \frac{|H_\gamma(\mu_h)|^2_{\rm NP}}{|H_\gamma(\mu_h)|^2_{\rm SM}} + \text{power corrections}. \tag{43}$$

The power corrections would introduce some mild dependence on the intermediate and low scales $\mu_{\rm i}$ and $\mu_0$, as well as on the cutoff $E_0$.

Another important example is the direct $CP$ asymmetry in $B \to X_s\gamma$ decays, for which we obtain

$$A_{CP} = \frac{\Gamma_{\bar{B}\to X_s\gamma} - \Gamma_{B\to X_{\bar{s}}\gamma}}{\Gamma_{\bar{B}\to X_s\gamma} + \Gamma_{B\to X_{\bar{s}}\gamma}} = \frac{|H_\gamma(\mu_h)|^2 - |\overline{H}_\gamma(\mu_h)|^2}{|H_\gamma(\mu_h)|^2 + |\overline{H}_\gamma(\mu_h)|^2} + \text{power corrections}, \tag{44}$$

where $\overline{H}_\gamma(\mu_h)$ is obtained by $CP$ conjugation, which in the standard model amounts to replacing $\varepsilon_{\rm CKM} \to \varepsilon_{\rm CKM}^*$ in (4). It follows that the predictions for the $CP$ asymmetry in the standard model and various new physics scenarios presented in [29] remain largely unaffected by our considerations.

### 7.2 Ratios sensitive to low-scale physics

The multi-scale effects studied in this work result from the fact that in practice the $B \to X_s\gamma$ decay rate is measured with a restrictive cut on the photon energy. As we have pointed out, this introduces sensitivity to the scales $\mu_{\rm i} \sim \sqrt{m_b\Delta}$ and $\mu_0 \sim \Delta = m_b - 2E_0$ in addition to the hard scale $\mu_h \sim m_b$. These complications would be absent if it were possible to measure the fully inclusive rate. It is

convenient to define a function $F(E_0)$ as the ratio of the $B \to X_s\gamma$ decay rate with a cut $E_0$ divided by the total rate,

$$F(E_0) = \frac{\Gamma_{\bar B\to X_s\gamma}(E_0)}{\Gamma_{\bar B\to X_s\gamma}(E_*)}\,. \tag{45}$$

Because of a logarithmic soft-photon divergence for very low energy, it is conventional to define the "total" inclusive rate as the rate with a very low cutoff $E_* = m_b/20$ [17]. The denominator in the expression for $F(E_0)$ can be evaluated using a conventional OPE, which corresponds to setting all three matching scales equal to $\mu_h$. The numerator is given by our expression in (20), supplemented by the power corrections in (40). We obtain

$$\begin{aligned} F(E_0) &= U_1(\mu_h,\mu_i)\,U_2(\mu_i,\mu_0)\,\frac{\mathrm{e}^{-\gamma_E\eta}}{\Gamma(1+\eta)}\left(\frac{\Delta}{\mu_0}\right)^{\eta} \\ &\quad\times\left(\mathcal{D}(\Delta)\left[p_3(\eta,\delta)+\frac{\eta(\eta-1)}{2}\,\frac{(-\lambda_1)}{3\Delta^2}\right]\right. \\ &\quad\left.+p_3(\eta,\delta)\,\frac{C_F\alpha_s(\mu_i)}{4\pi}\right. \\ &\quad\left.\times\sum_{i\le j}\mathrm{Re}\,\frac{C_i^*(\mu_h)\,C_j(\mu_h)}{|C_{7\gamma}^{\rm eff}(\mu_h)|^2}\,F_{ij}(\eta,\delta)\right) \\ &\quad\Bigg/\left(1+\frac{C_F\alpha_s(\mu_h)}{4\pi}\right. \\ &\quad\left.\times\left[\mathcal{H}(\delta_*)+\sum_{i\le j}\mathrm{Re}\,\frac{C_i^*(\mu_h)\,C_j(\mu_h)}{|C_{7\gamma}^{\rm eff}(\mu_h)|^2}\,\hat f_{ij}(\delta_*)\right]\right)\,, \end{aligned} \tag{46}$$

where $\delta = \Delta/m_b$, $\delta_* = 1 - 2E_*/m_b = 0.9$, and

$$\mathcal{D}(\Delta) = 1 + \frac{C_F\alpha_s(\mu_i)}{4\pi}\,\mathcal{J}(\Delta) + \frac{C_F\alpha_s(\mu_0)}{4\pi}\,\mathcal{S}(\Delta)\,, \tag{47}$$

$$\begin{aligned} \mathcal{H}(\delta_*) &= 4\ln^2\frac{m_b}{\mu_h} - 10\ln\frac{m_b}{\mu_h} - 2\ln^2\delta_* - 7\ln\delta_* + 7 \\ &\quad - \frac{7\pi^2}{6} + \delta_*\,(12\ln\delta_* + 9) - \delta_*^2\left(6\ln\delta_* + \frac{15}{2}\right) \\ &\quad + \delta_*^3\left(\frac{4}{3}\ln\delta_* + \frac{17}{9}\right) + \left(2\ln\delta_* + \frac{3}{2}\right)\frac{(-\lambda_1)}{3\delta_*^2 m_b^2}\,. \end{aligned}$$

The result (46) is RG invariant and so (formally) independent of the three matching scales $\mu_h$, $\mu_i$, and $\mu_0$, and at leading power it is insensitive to the hard matching corrections contained in $H_\gamma(\mu_h)$. To an excellent approximation, the fraction function $F(E_0)$ therefore applies to the standard model as well as to any new physics scenario. Note also that the $b$-quark mass enters the expression for the fraction function only at the level of power corrections. The prefactor $m_b^3\,\overline{m}_b^2(\mu_h)$, which multiplies the total decay rate, cancels out in the ratio (45). Finally, we stress that the expression for $F(E_0)$ given above still refers to the pole scheme. It is necessary to eliminate the pole-scheme parameters $m_b$ and $\lambda_1$ in favor of physical parameters before using this result.

Another important example of a ratio that is largely insensitive to the hard matching contributions is the average photon energy defined as

$$\langle E_\gamma\rangle = \frac{\displaystyle\int_{E_0}^{M_B/2}\mathrm{d}E_\gamma\,E_\gamma\,\frac{\mathrm{d}\Gamma}{\mathrm{d}E_\gamma}}{\displaystyle\int_{E_0}^{M_B/2}\mathrm{d}E_\gamma\,\frac{\mathrm{d}\Gamma}{\mathrm{d}E_\gamma}}\,, \tag{48}$$

which has been proposed as a good way to measure the $b$-quark mass or, equivalently, the HQET parameter $\bar\Lambda$ [53,54]. The impact of shape-function effects on the theoretical prediction for this ratio has been studied in [17, 55] and was found to be significant. Here we study the average photon energy in the MSOPE region, where a model-independent prediction can be obtained. It is structurally different from the one obtained using the conventional OPE in the sense that contributions associated with different scales are disentangled from each other. We find (with $\delta = \Delta/m_b$)

$$\begin{aligned} \langle E_\gamma\rangle &= \frac{m_b}{2}\left(1 - \frac{\lambda_1+3\lambda_2}{2m_b^2}\right) \\ &\quad\times\left\{\frac{\mathcal{D}(\Delta)\,p_4(\eta,\delta)}{\mathcal{D}(\Delta)\,p_3(\eta,\delta)}\right. \\ &\quad\left.+\frac{C_F\alpha_s(\mu_i)}{4\pi}\sum_{\substack{i,j=1,7,8\\ i\le j}}\mathrm{Re}\,\frac{C_i^*(\mu_h)C_j(\mu_h)}{|C_{7\gamma}^{\rm eff}(\mu_h)|^2}\,d_{ij}(\delta)\right\}\,, \end{aligned} \tag{49}$$

where $p_4(\eta,\delta)$ is defined in (22), and

$$d_{ij}(\delta) = \int_0^\delta \mathrm{d}x\,\hat f_{ij}(x) - \delta\,\hat f_{ij}(\delta)\,. \tag{50}$$

Analytical expressions for the functions $d_{ij}(\delta)$ are given in Appendix C. They vanish quadratically for $\delta \to 0$ and so give very small contributions for realistic values of the cutoff. We therefore do not include RG resummation effects for these terms. The non-perturbative corrections involving the parameters $\lambda_1$ and $\lambda_2$ are taken from [4]. Note that the expression in brackets is a purely perturbative result free of hadronic parameters. When expanded in fixed-order perturbation theory, our result (49) reduces to an expression first obtained in [17].

We stress that the hard scale $\mu_h \sim m_b$ affects the average photon energy only via second-order power corrections. This shows that it is not appropriate to compute the quantity $\langle E_\gamma\rangle$ using a simple heavy-quark expansion at the scale $m_b$, which is however done in the conventional OPE approach [53, 54]. This observation is important, because information about moments of the $B \to X_s\gamma$ photon spectrum is sometimes used in global fits to determine the CKM matrix element $|V_{cb}|$ along with HQET parameters.

Keeping only the leading power corrections, which is a very good approximation, the above expression simplifies to

$$\langle E_\gamma\rangle = \frac{m_b}{2} - \frac{\Delta}{2(1+\eta)^2}\left[\eta(1+\eta) + \frac{C_F\alpha_s(\mu_i)}{\pi}\left(\ln\frac{m_b\Delta}{\mu_i^2} - h(\eta) - \frac{3}{4} - \frac{1}{1+\eta}\right) - \frac{2C_F\alpha_s(\mu_0)}{\pi}\left(\ln\frac{\Delta}{\mu_0} - h(\eta) + \frac{1}{2} - \frac{1}{1+\eta}\right)\right] + \dots \quad (51)$$

In this approximation, $\langle E_\gamma\rangle$ only depends on physics at the intermediate and low scales $\mu_i$ and $\mu_0$. The next-to-leading order perturbative corrections in this formula are numerically quite significant. For $E_0 = 1.8\,\text{GeV}$, and taking the default scale choices $\mu_i = \sqrt{m_b\Delta}$ and $\mu_0 = \Delta$, we find in the pole scheme (using $m_b^{\rm pole} = 4.8\,\text{GeV}$ for the purpose of illustration) $\langle E_\gamma\rangle \approx [2.27 + 0.29\alpha_s(\sqrt{m_b\Delta}) - 0.19\alpha_s(\Delta)]\,\text{GeV}$. Eliminating the pole mass $m_b$ in favor of the $b$-quark mass $m_b(\Delta,\Delta)$ defined in the shape-function scheme, we obtain $\langle E_\gamma\rangle \approx [2.222 + 0.254\alpha_s(\sqrt{m_b\Delta}) + 0.009\alpha_s(\Delta)]\,\text{GeV} \approx 2.30\,\text{GeV}$. When the $b$-quark mass is defined in the shape-function scheme, the average photon energy is numerically very close to $\frac{1}{2}m_b(\Delta,\Delta) \approx 2.33\,\text{GeV}$, meaning that the first term in (51) dominates. Note also that the correction proportional to the low-scale coupling $\alpha_s(\Delta)$ is largely reduced in this scheme, ensuring an improved perturbative behavior.

## 8 Numerical results

We are now ready to present the phenomenological implications of our findings. Table 1 contains a list of the input parameters entering the analysis together with their present uncertainties. We have inflated the error on $\lambda_1$ obtained by averaging the values quoted in [60, 61] from $0.06\,\text{GeV}^2$ to $0.20\,\text{GeV}^2$, taking into account that this parameter is affected by infra-red renormalon ambiguities [44, 45]. We vary the quark masses $m_c$ and $m_b$ independently, in which case $\sqrt{z} = m_c(\mu_h)/m_b(\mu_h) = 0.221 \pm 0.027$. Additional uncertainties related to the possibility that the proper normalization point for the charm-quark mass in penguin loop graphs may be significantly lower than the hard scale $\mu_h$ are considered part of the perturbative error.

**Table 1.** Compilation of input parameters entering the numerical analysis. The top-quark mass enters the expressions for the Wilson coefficients $C_i$. The strange-quark mass is required as an infra-red regulator in (37). Only the real part of $\varepsilon_{\rm CKM}$ is needed for the calculations in this work

| Parameter | Value | Source |
|---|---|---|
| $m_b(\mu_*,\mu_*)$ [GeV] | $4.65 \pm 0.07$ | [14] |
| $\mu_\pi^2(\mu_*,\mu_*)$ [GeV$^2$] | $0.27 \pm 0.07$ | [14] |
| $\overline{m}_b(\overline{m}_b)$ [GeV] | $4.25 \pm 0.08$ | [56] |
| $\overline{m}_c(\overline{m}_c)$ [GeV] | $1.25 \pm 0.15$ | [57] |
| $m_t^{\rm pole}$ [GeV] | $178.0 \pm 4.3$ | [58] |
| $m_s/m_b$ | 0.02 | [17] |
| $\tau_B$ [ps] | $1.604 \pm 0.016$ | [57] |
| $\alpha_s(M_Z)$ | $0.1187 \pm 0.0020$ | [57] |
| $\lvert V_{ts}^* V_{tb}\rvert$ [$10^{-3}$] | $40.4^{+1.4}_{-0.6}$ | [59] |
| $\text{Re}(\varepsilon_{\rm CKM})$ [$10^{-3}$] | $9.8^{+5.1}_{-4.2}$ | [59] |
| $\lambda_1$ [GeV$^2$] | $-0.25 \pm 0.20$ | [60, 61] |
| $\lambda_2$ [GeV$^2$] | 0.12 | $\frac{1}{4}(M_{B^*}^2 - M_B^2)$ |

The most important correlations between input parameters are implemented as follows. We consider the two $b$-quark masses $m_b(\mu_*,\mu_*)$ and $\overline{m}_b(\overline{m}_b)$ as being fully correlated and vary their values simultaneously. The same applies to the values of the parameters $\mu_\pi^2(\mu_*,\mu_*)$ and $\lambda_1$. Next, we use that the value of $m_b$ is strongly anti-correlated with that of $|V_{cb}|$, because the most precise determination of $m_b$ is obtained from the analysis of $B \to X_c\,l\,\nu$ decay distributions. A recent study in [62] quotes a correlation coefficient $c = -0.49$ between $m_b$ and $|V_{cb}|$. CKM unitarity ensures that $|V_{cb}|$ is to a very good approximation equal to the product $|V_{ts}^* V_{tb}|$, so that the same anti-correlation can be assumed between $m_b$ and $|V_{ts}^* V_{tb}|$.

Before presenting our results, we reiterate that to apply the formulae derived in this work we must first eliminate the parameters $m_b$ and $\lambda_1$ defined in the pole scheme in terms of physical parameters defined in the shape-function scheme (we do not eliminate $\lambda_1$ in the second-order power corrections in (2) and (49)), and then expand the answer consistently to $\mathcal{O}(\alpha_s)$, treating ratios such as $\alpha_s(\mu_i)/\alpha_s(\mu_h)$ and $\alpha_s(\mu_0)/\alpha_s(\mu_i)$ as $\mathcal{O}(1)$ parameters. This expansion is readily automatized. Throughout, we use the three-loop expression for the running coupling $\alpha_s(\mu)$ defined in the $\overline{\rm MS}$ scheme [57].

### 8.1 Partial $B \to X_s\gamma$ branching ratio

We begin by presenting predictions for the $CP$-averaged $B \to X_s\gamma$ branching fraction with a cutoff $E_\gamma \ge E_0$ applied on the photon energy measured in the $B$-meson rest frame. Lowering $E_0$ below 2 GeV is challenging experimentally. The first measurement with $E_0 = 1.8\,\text{GeV}$ has recently been reported by the Belle Collaboration [6]. It yields[1]

$$\text{Br}(B \to X_s\gamma)\big|_{E_0=1.8\,\text{GeV}} = (3.38 \pm 0.30 \pm 0.29)\cdot 10^{-4}\,,$$
$$\langle E_\gamma\rangle\big|_{E_0=1.8\,\text{GeV}} = (2.292 \pm 0.026 \pm 0.034)\,\text{GeV}\,. \quad (52)$$

For $E_0 = 1.8\,\text{GeV}$ we have $\Delta \approx 1.1\,\text{GeV}$, which is sufficiently large to apply the formalism developed in the present work. We will also present results for $E_0 = 1.6\,\text{GeV}$ because this value has been used in some theoretical studies, although it has not yet been achieved in an experiment.

[1] To obtain the first result we had to undo a theoretical correction accounting for the effects of the cut $E_\gamma > 1.8\,\text{GeV}$, which had been applied to the experimental data.

**Table 2.** $B \to X_s\gamma$ branching ratio with estimates of perturbative uncertainties obtained by variation of the matching scales, for three variants of the shape-function scheme. See text for explanation

| $E_0$ | Scheme | Br $[10^{-4}]$ | $\mu_h$ | $\mu_i$ | $\mu_0$ | Sum | Power Cors. | Combined |
|---|---|---|---|---|---|---|---|---|
| 1.8 GeV | RS 1 | 3.37 | $^{+0.02}_{-0.00}$ | $^{+0.25}_{-0.37}$ | $^{+0.41}_{-0.03}$ | $^{+0.48}_{-0.37}$ | $^{+0.12}_{-0.07}$ | $^{+0.49}_{-0.38}$ |
| | RS 2 | 3.38 | $^{+0.02}_{-0.00}$ | $^{+0.25}_{-0.37}$ | $^{+0.15}_{-0.18}$ | $^{+0.29}_{-0.41}$ | $^{+0.12}_{-0.07}$ | $^{+0.31}_{-0.42}$ |
| | RS 3 | 3.36 | $^{+0.02}_{-0.00}$ | $^{+0.25}_{-0.37}$ | $^{+0.18}_{-0.18}$ | $^{+0.30}_{-0.41}$ | $^{+0.12}_{-0.07}$ | $^{+0.32}_{-0.42}$ |
| 1.6 GeV | RS 1 | 3.47 | $^{+0.02}_{-0.00}$ | $^{+0.28}_{-0.39}$ | $^{+0.14}_{-0.01}$ | $^{+0.31}_{-0.39}$ | $^{+0.10}_{-0.05}$ | $^{+0.33}_{-0.39}$ |
| | RS 2 | 3.47 | $^{+0.02}_{-0.00}$ | $^{+0.28}_{-0.39}$ | $^{+0.13}_{-0.14}$ | $^{+0.31}_{-0.41}$ | $^{+0.10}_{-0.05}$ | $^{+0.33}_{-0.41}$ |
| | RS 3 | 3.48 | $^{+0.02}_{-0.00}$ | $^{+0.28}_{-0.39}$ | $^{+0.18}_{-0.13}$ | $^{+0.33}_{-0.41}$ | $^{+0.10}_{-0.05}$ | $^{+0.34}_{-0.41}$ |

(For comparison, the value $E_0 = 2.0\,\text{GeV}$ adopted in the CLEO analysis [5] implies $\Delta \approx 0.7\,\text{GeV}$, which we believe may be too low for a short-distance treatment.)

We first set all input parameters to their default values and study the dependence of the branching ratio on the three matching scales $\mu_h$, $\mu_i$, and $\mu_0$. The sensitivity of our predictions to variations of the matching scales provides an estimate of unknown higher-order perturbative corrections. We shall study three different version of the shape-function scheme for the definition of the $b$-quark mass and the kinetic-energy parameter $\mu_\pi^2$, as discussed in Sect. 5. In the first scheme (called "RS 1") we use the parameters $m_b(\Delta,\mu_0)$ and $\mu_\pi^2(\Delta,\mu_0)$ defined in (33). In the second scheme ("RS 2") we instead use $m_b(\mu_0,\mu_0)$ and $\mu_\pi^2(\mu_0,\mu_0)$ from (34). Finally, in the third scheme ("RS 3") we employ the parameters $m_b(\mu_*,\mu_*)$ and $\mu_\pi^2(\mu_*,\mu_*)$ renormalized at a fixed scale $\mu_* = 1.5\,\text{GeV}$, at which their values have been determined in [14]. In the schemes RS 1 and RS 2, these reference values are evolved to other scales using equations derived in [14].

The matching scales are independently varied about their default values $\mu_h = m_b$, $\mu_i = \sqrt{m_b\Delta}$, and $\mu_0 = \Delta$ by multiplying them with factors between 2/3 and 3/2. Thus, for $m_b = 4.7\,\text{GeV}$ and $E_0 = 1.8\,\text{GeV}$, we vary $\mu_h \in [3.13, 7.05]\,\text{GeV}$, $\mu_i \in [1.52, 3.41]\,\text{GeV}$, and $\mu_0 \in [0.73, 1.65]\,\text{GeV}$, while for $E_0 = 1.6\,\text{GeV}$ the latter two ranges are replaced by $\mu_i \in [1.77, 3.98]\,\text{GeV}$, and $\mu_0 \in [1.0, 2.25]\,\text{GeV}$. Together, this covers a conservative range of scales. The resulting variations of the branching ratio are shown in Table 2.

We observe an excellent stability of our predictions with respect to variations of the hard matching scale $\mu_h$. In fact, the sensitivity is so small that it cannot reasonably be taken as an indication of the size of higher-order terms in the expansion in powers of $\alpha_s(\mu_h)$. The sensitivity to variations of the intermediate matching scale $\mu_i$ is more pronounced. The numbers suggest that terms of order $\alpha_s^2(\mu_i)$ could impact the branching ratio at the 10% level, which appears entirely reasonable given that $\alpha_s(\mu_i) \approx 0.3$. The sensitivity to the low matching scale $\mu_0$ turns out to be rather small. The coefficient of the $\alpha_s(\mu_0)$ term depends on the scheme adopted for the definition of the parameters $m_b$ and $\mu_\pi^2$, and it appears that in the three schemes considered here this coefficient is numerically small. While it is not guaranteed that this feature will persist in higher orders, the observation of good stability at the scale $\mu_0$ suggests that the shape-function scheme captures the most important low-scale effects and absorbs them into the running $b$-quark mass and the parameter $\mu_\pi^2$. The column labeled "Sum" shows the combined uncertainty obtained by adding the three scale variations in quadrature. The next column, labeled "Power Cors.", gives an estimate of the perturbative uncertainty in our treatment of kinematic power corrections, as discussed in Sect. 6. It is obtained by studying two variants of the expression (40), one where we set $p_3 \to 1$ and $F_{ij} \to \hat{f}_{ij}$, and one where in addition we neglect all anomalous-dimension functions except those governed by $\Gamma_{\text{cusp}}$. In both cases, we obtain expressions that differ from (40) by terms that are beyond the accuracy of our calculation. The resulting changes in the branching ratio are the same in all schemes and range between 1.5 and 3.5%, corresponding to a 10–25% uncertainty in the size of the power-suppressed contributions themselves. Finally, the last column in the table shows our estimates for the total perturbative uncertainty in the prediction of the branching ratio, which we find to be of order 10%, significantly larger than previous estimates. For example, the authors of [7,27] argued in favor of a perturbative error of only 4% from scale variation (when $m_c/m_b$ is kept fixed).

The remaining uncertainties in our predictions are due to input parameter variations. They are essentially the same in the three renormalization schemes and are summarized in Table 3 for the case of RS 2. The last column shows the combined errors, added in quadrature. They are

**Table 3.** $B \to X_s\gamma$ branching ratio with estimates of theoretical uncertainties due to input parameter variations as listed in Table 1. The upper (lower) sign refers to increasing (decreasing) a given input parameter

| $E_0$ | Br $[10^{-4}]$ | $m_b$ | $m_c$ | $m_t$ | $\lvert V_{ts}^* V_{tb}\rvert$ | $\tau_B$ | $\alpha_s(M_Z)$ | Combined |
|---|---|---|---|---|---|---|---|---|
| 1.8 GeV | 3.38 | $^{+0.31}_{-0.30}$ | $\mp 0.10$ | $\pm 0.04$ | $^{+0.24}_{-0.10}$ | $\pm 0.03$ | $^{+0.07}_{-0.08}$ | $^{+0.32}_{-0.30}$ |
| 1.6 GeV | 3.48 | $^{+0.30}_{-0.28}$ | $^{-0.11}_{+0.10}$ | $\pm 0.04$ | $^{+0.24}_{-0.10}$ | $\pm 0.03$ | $\pm 0.10$ | $^{+0.32}_{-0.29}$ |

**Table 4.** $B \to X_s\gamma$ event fraction $F(E_0)$ with estimates of perturbative uncertainties obtained by variation of the matching scales, for three variants of the shape-function scheme. See text for explanation

| $E_0$ | Scheme | $F(E_0)$ [%] | $\mu_h$ | $\mu_{\rm i}$ | $\mu_0$ | Sum | Power Cors. | Combined |
|---|---|---|---|---|---|---|---|---|
| 1.8 GeV | RS 1 | 89.1 | $^{+2.4}_{-2.2}$ | $^{+1.4}_{-5.0}$ | $^{+2.4}_{-5.4}$ | $^{+3.6}_{-7.7}$ | $^{+4.7}_{-2.4}$ | $^{+5.9}_{-8.1}$ |
| | RS 2 | 89.1 | $^{+2.4}_{-2.3}$ | $^{+1.5}_{-5.0}$ | $^{+2.6}_{-4.0}$ | $^{+3.8}_{-6.8}$ | $^{+4.7}_{-2.4}$ | $^{+6.0}_{-7.2}$ |
| | RS 3 | 89.2 | $^{+2.5}_{-2.3}$ | $^{+1.3}_{-5.0}$ | $^{+2.5}_{-3.7}$ | $^{+3.8}_{-6.6}$ | $^{+4.6}_{-2.4}$ | $^{+6.0}_{-7.0}$ |
| 1.6 GeV | RS 1 | 93.1 | $^{+2.8}_{-2.6}$ | $^{+2.7}_{-5.7}$ | $^{+2.6}_{-2.3}$ | $^{+4.7}_{-6.7}$ | $^{+3.9}_{-1.9}$ | $^{+6.1}_{-7.0}$ |
| | RS 2 | 93.1 | $^{+2.8}_{-2.6}$ | $^{+2.7}_{-5.7}$ | $^{+2.4}_{-2.5}$ | $^{+4.6}_{-6.8}$ | $^{+3.9}_{-1.9}$ | $^{+6.0}_{-7.1}$ |
| | RS 3 | 93.1 | $^{+2.8}_{-2.6}$ | $^{+2.7}_{-5.7}$ | $^{+2.6}_{-2.3}$ | $^{+4.7}_{-6.7}$ | $^{+3.9}_{-1.9}$ | $^{+6.1}_{-7.0}$ |

dominated by the uncertainties in the $b$-quark mass and in $|V_{ts}|$, whose significant anti-correlation ($c = -0.49$) is taken into account in computing the total error. Parameter dependences not shown in the table have a negligible effect ($< 1\%$) on the branching ratio. Note that in contrast to previous authors we do not divide the theoretical expression for the $B \to X_s\gamma$ decay rate by a semileptonic rate, but present an absolute prediction for the branching ratio itself. Once the correlation between parameters is properly taken into account, normalizing $\Gamma(B \to X_s\gamma)$ to the semileptonic rate $\Gamma(B \to X\,l\,\nu)$ does not lead to a significant reduction of the theoretical uncertainties.

The above results can be combined into the new standard model predictions

$$\begin{aligned}
&\mathrm{Br}(B \to X_s\gamma)\Big|_{E_0=1.8\,\mathrm{GeV}} \\
&= (3.38\,^{+0.31}_{-0.42}\,[\mathrm{pert.}]\,^{+0.32}_{-0.30}\,[\mathrm{pars.}]) \times 10^{-4}\,, \\
&\mathrm{Br}(B \to X_s\gamma)\Big|_{E_0=1.6\,\mathrm{GeV}} \\
&= (3.47\,^{+0.33}_{-0.41}\,[\mathrm{pert.}]\,^{+0.32}_{-0.29}\,[\mathrm{pars.}]) \times 10^{-4}\,, \qquad (53)
\end{aligned}$$

where we use the mass renormalization scheme RS 2 as our default. The first error refers to the perturbative uncertainty and the second one to parameter variations. The first value is in excellent agreement with the experimental result (52). Comparing the two results, and naively assuming Gaussian errors, we find that[2]

$$\mathrm{Br}(B\to X_s\gamma)_{\rm exp} - \mathrm{Br}(B\to X_s\gamma)_{\rm SM} < 1.3\cdot 10^{-4} \;\; (95\%\;\mathrm{CL})\,. \qquad (54)$$

We stress that, mainly as a result of the enlarged theoretical uncertainty but also due to the use of more recent data, this bound is much weaker than the one derived in [7], where this difference was found to be less than $0.5 \cdot 10^{-4}$. Consequently, we obtain weaker constraints on new physics parameters. For instance, for the case of the type-II two-Higgs-doublet model, we may use the analysis of [63] to obtain the bound

$$m_{H^+} > \text{approx. } 200\,\mathrm{GeV} \quad (95\%\;\mathrm{CL})\,, \qquad (55)$$

which is significantly weaker than the constraints $m_{H^+} > 500\,\mathrm{GeV}$ (at 95% CL) and $m_{H^+} > 350\,\mathrm{GeV}$ (at 99% CL) found in [7]. To find the precise numerical value for the bound would require a dedicated analysis, which is beyond the scope of this paper.

[2] We do not use the CLEO data [5] in deriving this bound, because the choice $E_0 = 2\,\mathrm{GeV}$ does not allow for a model-independent treatment of the effects of the cut.

### 8.2 Event fraction $F(E_0)$

As an alternative way to discuss the effects of imposing the cut on the photon energy, we study the fraction function $F(E_0)$ defined in (45), which up to power corrections is insensitive to the short-distance physics encoded in the Wilson coefficients $C_i$. The sensitivity of $F(E_0)$ to scale variations is studied in Table 4, which is analogous to Table 2 for the branching ratio. We find that the fraction function exhibits a stronger sensitivity to the hard scale $\mu_h$ than the branching ratio, changing by about 3% as $\mu_h$ is varied between $2m_b/3$ and $3m_b/2$. The sensitivity to variations of the matching scales $\mu_{\rm i}$ and $\mu_0$ follows the same pattern as in the case of the branching ratio, but the variations are somewhat smaller in magnitude. Note that there is a difference between the function $F(E_0)$ and the branching ratio as far as the dependence on $\mu_0$ is concerned, because the factor $m_b^3$ present in (26) and (40) cancels in the ratio (46). Since in the shape-function scheme the pole mass $m_b$ is expanded in a series in $\alpha_{\rm s}(\mu_0)$, this has an effect on the perturbative expansion. Finally, the perturbative uncertainties in the calculation of the power-suppressed terms are again at the level of a few percent. Our estimate for the combined perturbative error is presented in the last column.

In contrast to the $B \to X_s\gamma$ branching ratio, the fraction function $F(E_0)$ is independent of several input parameters (i.e., $\overline{m}_b(\overline{m}_b)$, $|V_{ts}^*V_{tb}|$, $\tau_B$, $\lambda_{1,2}$, and $\varepsilon_{\rm CKM}$), and it shows a very weak sensitivity to variations of the remaining parameters. This is illustrated in Table 5, which summarizes the resulting theoretical uncertainties for the case of RS 2. The

**Table 5.** $B \to X_s\gamma$ event fraction $F(E_0)$ with estimates of theoretical uncertainties due to input parameter variations as listed in Table 1. The upper (lower) sign refers to increasing (decreasing) a given input parameter

| $E_0$ | $F(E_0)$ [%] | $m_b$ | $m_c$ | $\alpha_{\rm s}(M_Z)$ | $\mu_\pi^2$ | Combined |
|---|---|---|---|---|---|---|
| 1.8 GeV | 89.1 | $^{+0.8}_{-1.0}$ | $\pm 0.5$ | $^{-1.1}_{+0.9}$ | $\mp 0.3$ | $^{+1.3}_{-1.6}$ |
| 1.6 GeV | 93.1 | $\pm 0.3$ | $\pm 0.4$ | $\mp 0.5$ | $\mp 0.1$ | $^{+0.7}_{-0.8}$ |

**Table 6.** Scale dependence and parameter variations for the average photon energy in $B \to X_s\gamma$ decays. See text for explanation

| $\langle E_\gamma\rangle$ [MeV] | $\mu_h$ | $\mu_{\rm i}$ | $\mu_0$ | Comb. | $m_b(\mu_*,\mu_*)$ | $-\lambda_1$ | $\alpha_{\rm s}(M_Z)$ | Comb. |
|---|---|---|---|---|---|---|---|---|
| 2272 | $\pm1$ | $^{+19}_{-17}$ | $^{+48}_{-70}$ | $^{+51}_{-72}$ | $\pm37$ | $\pm10$ | $^{-7}_{+6}$ | $\pm39$ |

combined errors are of order 1% and thus almost negligible compared with the perturbative uncertainties.

In summary, we obtain

$$F(1.8\,\text{GeV}) = (89\,^{+6}_{-7}\,[\text{pert.}] \pm 1\,[\text{pars.}])\%\,,$$
$$F(1.6\,\text{GeV}) = (93\,^{+6}_{-7}\,[\text{pert.}] \pm 1\,[\text{pars.}])\%\,. \qquad (56)$$

This is the first time that these fractions have been computed in a model-independent way. The result corresponding to $E_0 = 1.8\,\text{GeV}$ may be compared with the values $(95.8\,^{+1.3}_{-2.9})\%$ and $(95 \pm 1)\%$ obtained from the study of shape-function models in [17] and [55], respectively. In these studies, perturbative uncertainties have been ignored. A calculation in the conventional OPE approach gives a similar result, $(95.2\,^{+1.3}_{-2.9})\%$ [7], where the authors took the error estimate from [17]. In the present work, we obtain a smaller central value with a larger uncertainty.

As mentioned in the Introduction, the fraction function $F(E_0)$ can be used to combine our study of multi-scale effects with other, independent calculations of the total $B \to X_s\gamma$ branching ratio, both in the standard model and in extensions of it. For instance, we may use the result $(3.70 \pm 0.31) \times 10^{-4}$ for the total branching ratio in the standard model obtained from [7,27] (where the error contains a 6.7% perturbative uncertainty) and combine it with (56) to find

$$\begin{aligned}&\text{Br}(B \to X_s\gamma)\Big|_{E_0=1.8\,\text{GeV}}\\ &= (3.30\,^{+0.31}_{-0.35}\,[\text{pert.}] \pm 0.17\,[\text{pars.}]) \times 10^{-4}\,,\\ &\text{Br}(B \to X_s\gamma)\Big|_{E_0=1.6\,\text{GeV}}\\ &= (3.44\,^{+0.32}_{-0.35}\,[\text{pert.}] \pm 0.17\,[\text{pars.}]) \times 10^{-4}\,. \qquad (57)\end{aligned}$$

Compared with (53), the perturbative uncertainty is reduced slightly. However, only the reduction in the $\mu_0$ dependence can be taken seriously, as the $\mu_{\rm i}$ dependence is formally the same in (53) and (57). The significant reduction of the parameter uncertainties is partly due to the fact that the authors of [7,27] take smaller parameter variations than those in Table 1. When (57) is used instead of (53) in deriving the upper bound for the difference $\text{Br}(B \to X_s\gamma)_{\rm exp} - \text{Br}(B \to X_s\gamma)_{\rm SM}$ in (54), then this bound is reduced slightly, to $1.2 \cdot 10^{-4}$.

As a final remark, we compare our results for the branching ratio with a cut at $E_0 = 1.6\,\text{GeV}$ in (53) and (57) with the benchmark value $(3.57 \pm 0.30) \times 10^{-4}$ corresponding to the most recent calculation [27] published prior to the present work. Our central values are about 3% lower and, more importantly, the total theoretical uncertainties we find are about 50% larger.

### 8.3 Average photon energy

The last quantity we wish to explore is the average photon energy. As discussed in Sect. 7.2, this quantity is almost insensitive to high-scale physics as well as to non-perturbative hadronic effects. However, it is very sensitive to the interplay of physics at the intermediate and low scales, as illustrated by the approximate relation (51). Our predictions for $\langle E_\gamma\rangle$ and its theoretical uncertainties are summarized in Table 6 for the case $E_0 = 1.8\,\text{GeV}$, corresponding to the cut employed in [6]. Since in this case the differences between the three variants of the shape-function scheme are insignificant, we only show results for RS 2. As expected, we find essentially no dependence on the hard matching scale, a modest dependence on the intermediate scale, and a more pronounced sensitivity to the low scale. The combined errors from scale variations are of order 50–70 MeV. The study of uncertainties due to parameter variations exhibits that the prime sensitivity is to the $b$-quark mass, which is expected, since $\langle E_\gamma\rangle = m_b/2 + \ldots$ to leading order. The next-important contribution to the error comes from the HQET parameter $\lambda_1$. The total error is about 40 MeV.

Combining these results, we have to a very good approximation

$$\langle E_\gamma\rangle\Big|_{E_0=1.8\,\text{GeV}} = (2.27\,^{+0.05}_{-0.07})\,\text{GeV} + \frac{\delta m_b}{2} - \frac{\delta\lambda_1}{4m_b}\,, \qquad (58)$$

where the error accounts for the perturbative uncertainty. The central values for the relevant input parameters are $m_b(\mu_*,\mu_*) = 4.65\,\text{GeV}$ and $\lambda_1 = -0.25\,\text{GeV}^2$, and the quantities $\delta m_b$ and $\delta\lambda_1$ parameterize possible deviations from these values. Our prediction is in excellent agreement with the Belle result in (52). This finding provides support to the value of the $b$-quark mass in the shape-function scheme extracted in [14]. We stress, however, that the large perturbative uncertainties in the formula for $\langle E_\gamma\rangle$ impose significant limitations on the precision with which $m_b$ can be extracted from a measurement of the average photon energy. Our estimate above implies a perturbative uncertainty of $\delta m_b[\text{pert.}] = {}^{+140}_{-100}\,\text{MeV}$ in the extracted value of $m_b$, which could only be reduced by means of higher-order calculations. This uncertainty is in addition to twice the experimental error in the measurement of $\langle E_\gamma\rangle$, which at present yields $\delta m_b[\text{exp.}] = 86\,\text{MeV}$.

## 9 Conclusions and outlook

In this work, we have performed the first systematic analysis of the inclusive decays $B \to X_s\gamma$ in the presence of a photon-energy cut $E_\gamma \ge E_0$, where $E_0$ is such that $\Delta = m_b - 2E_0$ can be considered large compared to $\Lambda_{\rm QCD}$, while

still $\Delta \ll m_b$. This is the region of interest to experiments at the $B$ factories. The first condition ($\Delta \gg \Lambda_{\rm QCD}$) ensures that a theoretical treatment without shape functions can be applied. However, the second condition ($\Delta \ll m_b$) means that this treatment is *not* a conventional heavy-quark expansion in powers of $\alpha_s(m_b)$ and $\Lambda_{\rm QCD}/m_b$. Instead, we have shown that three distinct short-distance scales are relevant in this region. They are the hard scale $m_b$, the hard-collinear scale $\sqrt{m_b\Delta}$, and the low scale $\Delta$. To separate the contributions associated with these scales requires a multi-scale operator product expansion (MSOPE), we which have constructed in this work.

Our approach allows us to study analytically the transition from the shape-function region, where $\Delta \sim \Lambda_{\rm QCD}$, into the MSOPE region, where $\Lambda_{\rm QCD} \ll \Delta \ll m_b$, into the region $\Delta = \mathcal{O}(m_b)$, where a conventional heavy-quark expansion can be applied. This is a significant improvement over previous work. For instance, it has sometimes been argued that exactly where the transition to a conventional heavy-quark expansion occurs is an empirical question, which cannot be answered theoretically. Our formalism provides a precise, quantitative answer to this question. In particular, for $B \to X_s\gamma$ with realistic cuts on the photon energy one is *not* in a region where a simple short-distance expansion at the scale $m_b$ can be justified. The precision that can be achieved in the prediction of the $B \to X_s\gamma$ branching ratio is, ultimately, determined by how well perturbative and non-perturbative corrections can be controlled at the lowest relevant scale $\Delta$, which in practice is of order 1 GeV. Consequently, we find larger theoretical uncertainties than previous authors. These uncertainties are dominated by yet unknown higher-order perturbative effects. Non-perturbative, hadronic effects at the scale $\Delta$ appear to be small and under control.

Our treatment of the $B \to X_s\gamma$ branching ratio includes a complete resummation of logarithms $\ln(\Delta/m_b)$ at next-to-next-to-leading order in renormalization-group improved perturbation theory. This level of precision has not been achieved before. Besides the calculations performed here and in [14, 18], we have used multi-loop calculations for the cusp anomalous dimension [33, 34], the anomalous dimension of the shape function [64] (which we have corrected; see Appendix A and also [65]), and the anomalous dimension of the leading-order current operator in soft-collinear effective theory [37]. These ingredients are needed in order to achieve a complete separation of the perturbative corrections controlled by the three couplings $\alpha_s(m_b)$, $\alpha_s(\sqrt{m_b\Delta})$, and $\alpha_s(\Delta)$, which differ in magnitude by about a factor 2. Our prediction for the $CP$-averaged $B \to X_s\gamma$ with a cut $E_0 = 1.8\,\text{GeV}$ is $\text{Br}(B \to X_s\gamma) = (3.38^{+0.31}_{-0.42}\,[\text{pert.}]\,^{+0.32}_{-0.30}\,[\text{pars.}]) \times 10^{-4}$. With this cut $(89^{+6}_{-7} \pm 1)\%$ of all events are contained. The theory uncertainty we estimate is significantly larger than that found by previous authors, and this fact has important implications for searches of new physics in radiative $B$ decays. Quite generally, the constraints on model parameter space have to be relaxed significantly. We have illustrated this fact with the example of the type-II two-Higgs-doublet model, for which we find that the lower bound on the charged-Higgs mass is reduced to approximately 200 GeV.

This is not the first time in the history of $B \to X_s\gamma$ calculations that issues of scale setting have changed the prediction and error estimate for the branching ratio. In [22], Czarnecki and Marciano have pointed out that the electromagnetic coupling $\alpha$ in the expression for the decay rate should be identified with the fine-structure constant (normalized at $q^2 = 0$), and not with $\alpha(m_b)$ renormalized at the scale of the heavy quark in the decay. This lowered the prediction for the branching ratio by about 5%. More recently, Gambino and Misiak have argued that the charm-quark mass, which enters the next-to-leading order corrections to the $B \to X_s\gamma$ rate via penguin loops, should be identified with a running mass $m_c(\mu)$ with $\mu \sim m_b$ rather than with the pole mass [7]. This observation increased the prediction for the branching ratio by about 8%, and at the same time it increased the error estimate associated with the value of the ratio $m_c/m_b$, which before had been taken to be the (rather well known) ratio of the two pole masses. The point we emphasize in the present work, namely that some effects in $B \to X_s\gamma$ decays should be described by the couplings $\alpha_s(\sqrt{m_b\Delta})$ and $\alpha_s(\Delta)$ (and power corrections at the scale $\Delta$) rather than $\alpha_s(m_b)$, is of a similar nature. However, in our case the change in perspective about the theory of $B \to X_s\gamma$ decay is more profound, as it imposes limitations on the very validity of a short-distance treatment. If the short-distance expansion at the scale $\Delta$ fails, then the rate *cannot* be calculated without resource to non-perturbative shape functions, which would introduce an irreducible amount of model dependence. In practice, while $\Delta \approx 1.1\,\text{GeV}$ (for $E_0 \approx 1.8\,\text{GeV}$) is probably sufficiently large to trust a short-distance analysis, it would be unreasonable to expect that yet unknown higher-order effects should be less important than in the case of other low-scale applications of QCD, such as in hadronic $\tau$ decays.

Given the prominent role of $B \to X_s\gamma$ decay in searching for physics beyond the standard model, it is of great importance to have a precise prediction for its rate in the standard model. The present work shows that the ongoing effort to calculate the dominant parts of the next-to-next-to-leading corrections in the conventional heavy-quark expansion is only part of what is needed to achieve this goal. Equally important will be to compute the dominant higher-order corrections of order $\alpha_s^2(\Delta)$ and $\alpha_s^2(\sqrt{m_b\Delta})$, and to perform a renormalization-group analysis of the leading kinematic power corrections of order $\Delta/m_b$. In fact, our error analysis suggests that these effects are potentially more important that the hard matching corrections at the scale $m_b$. Let us finish by mentioning two possible approaches for addressing the issue of higher-order perturbative effects at the intermediate and low scales: First, it would be interesting to calculate the terms of order $\beta_0\alpha_s^2$ at the scales $\mu_i \sim \sqrt{m_b\Delta}$ and $\mu_0 \sim \Delta$. While this would fall short of a complete calculation of $\mathcal{O}(\alpha_s^2)$ corrections, the "BLM terms" associated with the $\beta$ function are often numerically dominant [66,67]. We stress that the known $\mathcal{O}(\beta_0\alpha_s^2)$ terms computed in the conventional heavy-quark expansion [54]

are not sufficient for this purpose. Separate computations of $\mathcal{O}(\beta_0\alpha_s^2)$ terms at the scales $\mu_h \sim m_b$, $\mu_i \sim \sqrt{m_b\Delta}$, and $\mu_0 \sim \Delta$ would be required to perform a meaningful BLM scale setting. This statement is explained in Appendix D. Secondly, the convergence of the perturbative expansion at the low scale $\mu_0 \sim \Delta$ may be improved by borrowing the idea of "contour resummation" developed in [68]. Since the shape-function integrals can be written as contour integrals in the complex plane along a circle with radius $\Delta$, in may be more appropriate to use a contour-weighted coupling constant rather than the naive coupling $\alpha_s(\Delta)$. Exploring the numerical impact of these two proposals is left for future work.

*Acknowledgements.* I am grateful to Joan Soto and Domenec Espriu for their hospitality during a visit to the Departament d'Estructura i Constituents de la Matèria at Universitat de Barcelona, Spain, where part of this work was performed. It is a pleasure to thank Björn Lange, Xavier Garcia i Tormo, and Ignazio Scimemi for useful discussions. I am grateful to Gregory Korchemsky for bringing the paper [38] to my attention, and for discussions concerning the two-loop anomalous dimension of the shape function. Finally, I am indebted to Einan Gardi for providing the perturbative expansion of his expression for the $B \to X_s\gamma$ rate obtained in [36], and for many illuminating discussions of factorization results in deep-inelastic scattering, which have been instrumental in finding the (hopefully correct) expressions for the two-loop anomalous dimensions presented in Appendix A. This research was supported by the National Science Foundation under Grant PHY-0355005.

## Appendix A: Anomalous dimensions and RG functions

The exact solutions (14) to the RG equations in (12) can be evaluated perturbatively by expanding the anomalous dimensions and $\beta$ function,

$$\Gamma_{\rm cusp}(\alpha_s) = \Gamma_0\,\frac{\alpha_s}{4\pi} + \Gamma_1\left(\frac{\alpha_s}{4\pi}\right)^2 + \Gamma_2\left(\frac{\alpha_s}{4\pi}\right)^3 + \dots\,, \quad \text{(A.1)}$$
$$\beta(\alpha_s) = -2\alpha_s\left[\beta_0\,\frac{\alpha_s}{4\pi} + \beta_1\left(\frac{\alpha_s}{4\pi}\right)^2 + \beta_2\left(\frac{\alpha_s}{4\pi}\right)^3 + \dots\right],$$

and similarly for the remaining anomalous dimensions. We work consistently at next-to-leading order in RG-improved perturbation theory, keeping terms through order $\alpha_s$ in the final expressions for the Sudakov exponent $S$ and the functions $a_\Gamma$, $a_\gamma$, and $a_{\gamma'}$. For $a_\Gamma$ one obtains the standard expression

$$a_\Gamma(\nu,\mu) \quad \text{(A.2)}$$
$$= \frac{\Gamma_0}{2\beta_0}\left[\ln\frac{\alpha_s(\mu)}{\alpha_s(\nu)} + \left(\frac{\Gamma_1}{\Gamma_0} - \frac{\beta_1}{\beta_0}\right)\frac{\alpha_s(\mu)-\alpha_s(\nu)}{4\pi} + \dots\right].$$

The result for the Sudakov factor $S$ is more complicated, as it is necessary to include terms of next-to-next-to-leading logarithmic order. We obtain

$$\begin{aligned} S(\nu,\mu) = \frac{\Gamma_0}{4\beta_0^2}\,\Bigg\{ & \frac{4\pi}{\alpha_s(\nu)}\left(1-\frac{1}{r}-\ln r\right) \\ & + \left(\frac{\Gamma_1}{\Gamma_0} - \frac{\beta_1}{\beta_0}\right)(1-r+\ln r) + \frac{\beta_1}{2\beta_0}\ln^2 r \\ & + \frac{\alpha_s(\nu)}{4\pi}\left[\left(\frac{\beta_1\Gamma_1}{\beta_0\Gamma_0} - \frac{\beta_2}{\beta_0}\right)(1-r+r\ln r)\right. \\ & + \left(\frac{\beta_1^2}{\beta_0^2} - \frac{\beta_2}{\beta_0}\right)(1-r)\ln r \\ & \left. - \left(\frac{\beta_1^2}{\beta_0^2} - \frac{\beta_2}{\beta_0} - \frac{\beta_1\Gamma_1}{\beta_0\Gamma_0} + \frac{\Gamma_2}{\Gamma_0}\right)\frac{(1-r)^2}{2}\right] \\ & + \dots\Bigg\}, \end{aligned} \quad \text{(A.3)}$$

where $r = \alpha_s(\mu)/\alpha_s(\nu)$. Whereas the two-loop anomalous dimensions and $\beta$ function are required in (A.2), the expression for $S$ also involves the three-loop coefficients $\Gamma_2$ and $\beta_2$.

The perturbative expansion of the QCD $\beta$ function to three-loop order is [69] (all results refer to the $\overline{\rm MS}$ renormalization scheme)

$$\begin{aligned} \beta_0 &= \frac{11}{3}\,C_A - \frac{2}{3}\,n_f = \frac{25}{3}\,, \\ \beta_1 &= \frac{34}{3}\,C_A^2 - \frac{10}{3}\,C_A\,n_f - 2C_F\,n_f = \frac{154}{3}\,, \\ \beta_2 &= \frac{2857}{54}\,C_A^3 + \left(C_F^2 - \frac{205}{18}\,C_FC_A - \frac{1415}{54}\,C_A^2\right)n_f \\ &\quad + \left(\frac{11}{9}\,C_F + \frac{79}{54}\,C_A\right)n_f^2 = \frac{21943}{54}\,, \end{aligned} \quad \text{(A.4)}$$

where the numerical values refer to $N_c = 3$ and $n_f = 4$. The two-loop coefficient of the cusp anomalous dimension has been known for a long time [33]. However, its three-loop coefficient has only been calculated very recently by Moch et al. [34]. This is a lucky coincidence, because that calculation was done in a context not related to heavy-quark physics. The results are

$$\begin{aligned} \Gamma_0 &= 4C_F = \frac{16}{3}\,, \\ \Gamma_1 &= 8C_F\left[\left(\frac{67}{18} - \frac{\pi^2}{6}\right)C_A - \frac{5}{9}\,n_f\right] \approx 42.7695\,, \\ \Gamma_2 &= 16C_F\left[\left(\frac{245}{24} - \frac{67\pi^2}{54} + \frac{11\pi^4}{180} + \frac{11}{6}\,\zeta_3\right)C_A^2\right. \\ &\quad + \left(-\frac{209}{108} + \frac{5\pi^2}{27} - \frac{7}{3}\,\zeta_3\right)C_A\,n_f \\ &\quad \left. + \left(-\frac{55}{24} + 2\zeta_3\right)C_F\,n_f - \frac{1}{27}\,n_f^2\right] \approx 429.507\,. \end{aligned} \quad \text{(A.5)}$$

Although the two- and three-loop coefficients of the $\beta$ function and cusp anomalous dimension are large, the perturbative expansion of the Sudakov exponent is extremely well behaved. This is illustrated in Fig. 3, which shows the Sudakov exponents $S(\mu_h,\mu)$ and $S(\mu_0,\mu)$ for $\mu_h = m_b = 4.7\,\text{GeV}$ and $\mu_0 = 1\,\text{GeV}$ as a function of $\mu$.

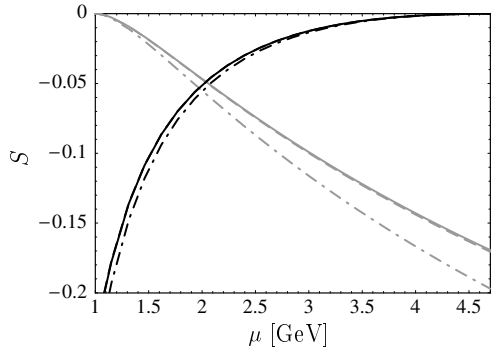


**Fig. 3.** Sudakov exponents $S(m_b,\mu)$ (black) and $S(1\,\text{GeV},\mu)$ (gray) at next-to-next-to-leading order (solid), next-to-leading order (dashed), and leading order (dash-dotted). The solid and dashed curves are nearly indistinguishable

The two-loop coefficient of the anomalous dimension $\gamma$ entering the shape-function evolution kernel in (17) has been calculated in [64]. We have found some mistakes in the translation of the results for the two-loop graphs into the expression for the anomalous dimension. The corrected result is[3]

$$\begin{aligned}\gamma_0 &= -2C_F = -\frac{8}{3}\,,\\ \gamma_1 &= -8C_F\left[\left(-\frac{37}{108}-\frac{\pi^2}{144}+\frac{9}{4}\,\zeta_3-\frac{\kappa}{8}\right)C_A\right.\\ &\quad\left.-\left(\frac{1}{54}+\frac{\pi^2}{72}\right)n_f\right]\approx -66.7531+4\kappa\,,\end{aligned}\tag{A.6}$$

where $\kappa = 0$ under the assumption that the two-loop diagrams themselves were evaluated correctly in [64]. However, there is reason to believe that there might be an additional error in this paper, giving rise to a non-zero value $\kappa = 4/3$ [65] (see also Appendix B below), which we adopt in our numerical analysis.

The two-loop anomalous dimension for the leading-order SCET current operator in (13) has not yet been computed directly. An analysis is in progress and has already led to a prediction for the terms of order $C_F n_f$ [37]. The remaining terms can be deduced by noting that the difference $\gamma^J \equiv \gamma' - \gamma$ is the non-cusp part of the anomalous dimension of the jet function [12], which is related to the familiar jet function from deep-inelastic scattering. We find

$$\begin{aligned}\gamma_0^J &= -3C_F\,,\\ \gamma_1^J &= C_F\left[\left(-\frac{3}{2}+2\pi^2-24\zeta_3\right)C_F\right.\\ &\quad+\left(-\frac{3155}{54}+\frac{22\pi^2}{9}+40\zeta_3\right)C_A\\ &\quad\left.+\left(\frac{247}{27}-\frac{4\pi^2}{9}\right)n_f\right]+(7-\pi^2)C_F\beta_0\,,\end{aligned}\tag{A.7}$$

where the terms in brackets in the expression for $\gamma_1^J$ are taken from [35], while the remainder in the last line is due to the non-trivial normalization of the SCET jet function in (9). Combining the results (A.6) and (A.7), we obtain

$$\begin{aligned}\gamma_0' &= -5C_F = -\frac{20}{3}\,,\\ \gamma_1' &= -8C_F\left[\left(\frac{3}{16}-\frac{\pi^2}{4}+3\zeta_3\right)C_F\right.\\ &\quad+\left(\frac{1621}{432}+\frac{7\pi^2}{48}-\frac{11}{4}\,\zeta_3-\frac{\kappa}{8}\right)C_A\\ &\quad\left.-\left(\frac{125}{216}+\frac{\pi^2}{24}\right)n_f\right]\approx -36.9764+4\kappa\,.\end{aligned}\tag{A.8}$$

Only the term proportional to $n_f$ in $\gamma_1'$ has so far been checked by a direct calculation in SCET [37].

## Appendix B: Perturbative expansion

In this work, we have presented for the first time the complete RG-improved expression for the $B \to X_s\gamma$ decay rate, in which all logarithms $\ln\delta$ (with $\delta = \Delta/m_b$) are resummed at next-to-next-to-leading logarithmic order. In order to simplify the comparison of our result with those of other authors, we expand it in fixed-order perturbation theory and list the resulting terms at order $\alpha_s$ and $\alpha_s^2$. It suffices to focus on the perturbative correction to the term multiplying the product $m_b^3\,\overline{m}_b^2(\mu_h)\,|C_{7\gamma}(\mu_h)|^2$, where $m_b$ is the pole mass. We find

$$\begin{aligned}1\ &+C_F\,\frac{\alpha_s(m_b)}{4\pi}\left(4\ln\frac{m_b}{\mu_h}-2\ln^2\delta-7\ln\delta-5-\frac{4\pi^2}{3}\right)\\ &+C_F\left(\frac{\alpha_s(m_b)}{4\pi}\right)^2\\ &\times\left[k_4\ln^4\delta+k_3\ln^3\delta+k_2\ln^2\delta+k_1\ln\delta+k_0\right]+\dots\,,\end{aligned}\tag{B.1}$$

where

$$\begin{aligned}k_4 &= 2C_F\,,\qquad k_3 = 14C_F+\frac{22}{3}\,C_A-\frac{4}{3}\,n_f\,,\\ k_2 &= \left(-8\ln\frac{m_b}{\mu_h}+\frac{69}{2}+\frac{4\pi^2}{3}\right)C_F+\left(\frac{95}{18}+\frac{2\pi^2}{3}\right)C_A\\ &\quad-\frac{13}{9}\,n_f\,,\\ k_1 &= \left(-28\ln\frac{m_b}{\mu_h}+\frac{67}{2}+\frac{20\pi^2}{3}-8\zeta_3\right)C_F\\ &\quad+\left(2\kappa-\frac{953}{18}+\frac{34\pi^2}{9}+4\zeta_3\right)C_A+\left(\frac{85}{9}-\frac{4\pi^2}{9}\right)n_f\,.\end{aligned}\tag{B.2}$$

These expressions are independent of the matching scales $\mu_i$ and $\mu_0$, and they have the correct dependence on $\mu_h$. The constant $k_0$ can only be obtained from a complete calculation of $\mathcal{O}(\alpha_s^2)$ corrections to the decay rate.

[3] I am grateful to G. Korchemsky for confirming my result [70].

Resummed expressions for the $B \to X_s\gamma$ photon spectrum with next-to-leading logarithmic accuracy have been reported in [71] and [36]. In the first paper, expressions for the coefficients $k_4$ and $k_3$ are derived, which agree with our findings. In [36], Gardi has obtained a result for the photon spectrum from which all four coefficients $k_i$ can be extracted. By matching his result for $k_1$ with ours, we conclude that $\kappa = 4/3$.

## Appendix C: Kinematic power corrections for the average photon energy

The functions $d_{ij}(\delta)$ entering the expression for the average photon energy in (49) are given by

$$\begin{aligned}
d_{77}(\delta) &= \left(8\delta^2 - \frac{14\delta^3}{3} + \delta^4\right)\ln\delta + \frac{7\delta^2}{2} - \frac{58\delta^3}{9} + 2\delta^4\,,\\
d_{88}(\delta) &= \frac{4}{9}\left[\frac{\pi^2}{6} - L_2(1-\delta) + \left(\delta + \frac{\delta^2}{4} + \frac{\delta^3}{6}\right)\ln\delta\right.\\
&\quad \left. - \delta - \frac{\delta^2}{4} - \frac{5\delta^3}{36} + \frac{\delta^4}{8}\right]\\
&\quad + \frac{8}{9}\left(\ln\frac{m_b}{m_s} - 1\right)\left[\ln(1-\delta) + \delta + \frac{\delta^2}{4} + \frac{\delta^3}{6}\right],\\
d_{78}(\delta) &= \frac{8}{3}\left[\frac{\pi^2}{6} - L_2(1-\delta) + \left(\delta + \frac{\delta^2}{2}\right)\ln\delta - \delta\right.\\
&\quad \left. - \frac{7\delta^2}{8} + \frac{\delta^3}{6} - \frac{\delta^4}{16}\right],\\
d_{11}(\delta) &= -\frac{8}{9}\int_0^1 \mathrm{d}x\,(1-x)(1-x_\delta)^2\left|\frac{z}{x}\,G\Big(\frac{x}{z}\Big) + \frac{1}{2}\right|^2,\\
d_{17}(\delta) &= -3d_{18}(\delta)\\
&= \frac{4}{3}\int_0^1 \mathrm{d}x\,x(1-x_\delta)^2\,\mathrm{Re}\left[\frac{z}{x}\,G\Big(\frac{x}{z}\Big) + \frac{1}{2}\right], \quad \text{(C.1)}
\end{aligned}$$

where $x_\delta = \max(x, 1-\delta)$, $z = (m_c/m_b)^2$, and the function $G(t)$ has been defined in (38).

## Appendix D: Comment on BLM scale setting

Here we illustrate the simple fact that the BLM scale-setting procedure [66] for multi-scale problems is more complicated than in the familiar case with a single scale. Let us, for simplicity, ignore RG resummation effects due to anomalous dimensions and consider a physical quantity $A$, whose perturbative expansion is given by the product of two perturbative series at scales $M$ and $m$, with $M > m$. We write

$$\begin{aligned}
A &= \left[1 + c_1\,a(M) + (2\beta_0 c_2 + c_2')\,a^2(M) + \ldots\right]\\
&\quad \times \left[1 + d_1\,a(m) + (2\beta_0 d_2 + d_2')\,a^2(m) + \ldots\right], \quad \text{(D.1)}
\end{aligned}$$

where $a \equiv \alpha_s/(4\pi)$, and $c_i^{(\prime)}$, $d_i^{(\prime)}$ are numerical coefficients. The BLM scales of the two series are

$$\mu_{\rm BLM}^{\rm high} = M\,\mathrm{e}^{-c_2/c_1}\,, \qquad \mu_{\rm BLM}^{\rm low} = m\,e^{-d_2/d_1}\,. \quad \text{(D.2)}$$

They are determined so as to absorb the $\mathcal{O}(\alpha_s^2)$ terms multiplying $\beta_0$ into the running coupling constants. Adopting the BLM philosophy, we would conclude that perturbation theory is well behaved as long as both $\mu_{\rm BLM}^{\rm high}$ and $\mu_{\rm BLM}^{\rm low}$ are in the perturbative regime.

Imagine now that we compute $A$ in fixed-order perturbation theory using a single coupling constant $\alpha_s(\mu)$. We would obtain

$$\begin{aligned}
A &= 1 + (c_1 + d_1)\,a(\mu)\\
&\quad + \left[2\beta_0\left(c_2 + d_2 - c_1\ln\frac{M}{\mu} - d_1\ln\frac{m}{\mu}\right)\right.\\
&\quad \left. + (c_2' + d_2' + c_1 d_1)\right]a^2(\mu) + \ldots\,, \quad \text{(D.3)}
\end{aligned}$$

and the associated BLM scale would be

$$\mu_{\rm BLM}^{\rm avg} = M\left(\frac{m}{M}\right)^{d_1/(c_1+d_1)}\exp\left(-\frac{c_2+d_2}{c_1+d_1}\right). \quad \text{(D.4)}$$

Obviously, (D.3) does not provide the same information as (D.1), and in particular it does not allow us to compute the BLM scales in (D.2). To this end we would need $c_2$ and $d_2$ separately, not just their sum.

It is instructive to look at a couple of examples, where the conclusions derived from (D.3) would differ strongly from those derived from (D.1). Consider, for instance, a situation where $(c_1 + d_1)$ is accidentally small. Then the BLM scale (D.4) is either very small or very large, whereas the BLM scales in (D.2) could be close to the scales $M$ and $m$, respectively. BLM scale setting based on the fixed-order calculation would then be totally misleading. Next, consider the case where the coefficient of $\beta_0$ in (D.3) is small, for instance by a particular choice of $\mu$. The fixed-order calculation would lead us to conclude that BLM-type corrections are small, whereas the BLM-type terms in (D.1) could still be large. Finally, consider the (somewhat pathological) example where $d_1 \simeq c_1$ and $d_2 \simeq -c_2$ with $\gamma = d_2/d_1 > 0$. Then the "physical" BLM scales are $\mu_{\rm BLM}^{\rm high} \simeq \mathrm{e}^{\gamma} M$ and $\mu_{\rm BLM}^{\rm low} \simeq \mathrm{e}^{-\gamma}\,m$. If $\gamma$ is large, perturbation theory may be in trouble, since $\mu_{\rm BLM}^{\rm low}$ may no longer be in the perturbative regime. Nevertheless, the "average" BLM scale $\mu_{\rm BLM}^{\rm avg} \simeq \sqrt{Mm}$ is large, and the fixed-order calculation would thus indicate a well-behaved perturbative expansion.

## References

1. For a review, see T. Hurth, Rev. Mod. Phys. **75**, 1159 (2003) [hep-ph/0212304]
2. K. Bieri, C. Greub, M. Steinhauser, Phys. Rev. D **67**, 114019 (2003) [hep-ph/0302051]
3. M. Misiak, M. Steinhauser, Nucl. Phys. B **683**, 277 (2004) [hep-ph/0401041]

4. A.F. Falk, M.E. Luke, M.J. Savage, Phys. Rev. D **49**, 3367 (1994) [hep-ph/9308288]
5. S. Chen et al. [CLEO Collaboration], Phys. Rev. Lett. **87**, 251807 (2001) [hep-ex/0108032]
6. P. Koppenburg et al. [Belle Collaboration], Phys. Rev. Lett. **93**, 061803 (2004) [hep-ex/0403004]
7. P. Gambino, M. Misiak, Nucl. Phys. B **611**, 338 (2001) [hep-ph/0104034]
8. M. Neubert, Phys. Rev. D **49**, 3392 (1994) [hep-ph/9311325]; D **49**, 4623 (1994) [hep-ph/9312311]
9. I.I.Y. Bigi, M.A. Shifman, N.G. Uraltsev, A.I. Vainshtein, Int. J. Mod. Phys. A **9**, 2467 (1994) [hep-ph/9312359]
10. T. Mannel, M. Neubert, Phys. Rev. D **50**, 2037 (1994) [hep-ph/9402288]
11. A.F. Falk, E. Jenkins, A.V. Manohar, M.B. Wise, Phys. Rev. D **49**, 4553 (1994) [hep-ph/9312306]
12. G.P. Korchemsky, G. Sterman, Phys. Lett. B **340**, 96 (1994) [hep-ph/9407344]
13. R. Akhoury, I.Z. Rothstein, Phys. Rev. D **54**, 2349 (1996) [hep-ph/9512303]
14. S.W. Bosch, B.O. Lange, M. Neubert, G. Paz, Nucl. Phys. B **699**, 335 (2004) [hep-ph/0402094]
15. C.W. Bauer, A.V. Manohar, Phys. Rev. D **70**, 034024 (2004) [hep-ph/0312109]
16. R.D. Dikeman, M.A. Shifman, N.G. Uraltsev, Int. J. Mod. Phys. A **11**, 571 (1996) [hep-ph/9505397]
17. A.L. Kagan, M. Neubert, Eur. Phys. J. C **7**, 5 (1999) [hep-ph/9805303]
18. B.O. Lange, M. Neubert, Phys. Rev. Lett. **91**, 102001 (2003) [hep-ph/0303082]
19. C.W. Bauer, S. Fleming, D. Pirjol, I.W. Stewart, Phys. Rev. D **63**, 114020 (2001) [hep-ph/0011336]; C.W. Bauer, D. Pirjol, I.W. Stewart, Phys. Rev. D **65**, 054022 (2002) [hep-ph/0109045]
20. For a review, see M. Neubert, Phys. Rept. **245**, 259 (1994) [hep-ph/9306320]
21. E. Braaten, S. Narison, A. Pich, Nucl. Phys. B **373**, 581 (1992)
22. A. Czarnecki, W.J. Marciano, Phys. Rev. Lett. **81**, 277 (1998) [hep-ph/9804252]
23. S.W. Bosch, R.J. Hill, B.O. Lange, M. Neubert, Phys. Rev. D **67**, 094014 (2003) [hep-ph/0301123]
24. M. Beneke, G. Buchalla, M. Neubert, C.T. Sachrajda, Nucl. Phys. B **606**, 245 (2001) [hep-ph/0104110]
25. K.G. Chetyrkin, M. Misiak, M. Münz, Phys. Lett. B **400**, 206 (1997) [Erratum B **425**, 414 (1998)] [hep-ph/9612313]
26. C. Greub, T. Hurth, D. Wyler, Phys. Rev. D **54**, 3350 (1996) [hep-ph/9603404]
27. A.J. Buras, A. Czarnecki, M. Misiak, J. Urban, Nucl. Phys. B **631**, 219 (2002) [hep-ph/0203135]
28. J.M. Soares, Nucl. Phys. B **367**, 575 (1991)
29. A.L. Kagan, M. Neubert, Phys. Rev. D **58**, 094012 (1998) [hep-ph/9803368]
30. P. Gambino, U. Haisch, JHEP **0009**, 001 (2000) [hep-ph/0007259]
31. K. Baranowski, M. Misiak, Phys. Lett. B **483**, 410 (2000) [hep-ph/9907427]
32. F. De Fazio, M. Neubert, JHEP **9906**, 017 (1999) [hep-ph/9905351]
33. G.P. Korchemsky, A.V. Radyushkin, Nucl. Phys. B **283**, 342 (1987); I.A. Korchemskaya, G.P. Korchemsky, Phys. Lett. B **287**, 169 (1992)
34. S. Moch, J.A.M. Vermaseren, A. Vogt, Nucl. Phys. B **688**, 101 (2004) [hep-ph/0403192]
35. A. Vogt, Phys. Lett. B **497**, 228 (2001) [hep-ph/0010146]
36. E. Gardi, JHEP **0404**, 049 (2004) [hep-ph/0403249]; E. Gardi, R.G. Roberts, Nucl. Phys. B **653**, 227 (2003) [hep-ph/0210429], and unpublished work
37. X. Garcia i Tormo, M. Neubert, I. Scimemi, in preparation
38. A.G. Grozin, G.P. Korchemsky, Phys. Rev. D **53**, 1378 (1996) [hep-ph/9411323]
39. C. Balzereit, T. Mannel, W. Kilian, Phys. Rev. D **58**, 114029 (1998) [hep-ph/9805297]
40. C.W. Bauer, M.E. Luke, T. Mannel, Phys. Rev. D **68**, 094001 (2003) [hep-ph/0102089]
41. M. Neubert, T. Becher, Phys. Lett. B **535**, 127 (2002) [hep-ph/0105217]
42. I.I.Y. Bigi, M.A. Shifman, N.G. Uraltsev, A.I. Vainshtein, Phys. Rev. D **50**, 2234 (1994) [hep-ph/9402360]
43. M. Beneke, V.M. Braun, Nucl. Phys. B **426**, 301 (1994) [hep-ph/9402364]
44. G. Martinelli, M. Neubert, C.T. Sachrajda, Nucl. Phys. B **461**, 238 (1996) [hep-ph/9504217]
45. M. Neubert, Phys. Lett. B **393**, 110 (1997) [hep-ph/9610471]
46. A. Ali, C. Greub, Phys. Lett. B **361**, 146 (1995) [hep-ph/9506374]
47. R.J. Hill, T. Becher, S.J. Lee, M. Neubert, JHEP **0407**, 081 (2004) [hep-ph/0404217]
48. T. Becher, R.J. Hill, B.O. Lange, M. Neubert, Phys. Rev. D **69**, 034013 (2004) [hep-ph/0309227]
49. M.B. Voloshin, Phys. Lett. B **397**, 275 (1997) [hep-ph/9612483]
50. Z. Ligeti, L. Randall, M.B. Wise, Phys. Lett. B **402**, 178 (1997) [hep-ph/9702322]
51. A. Kapustin, Z. Ligeti, H.D. Politzer, Phys. Lett. B **357**, 653 (1995) [hep-ph/9507248]
52. T. Becher, S. Braig, M. Neubert, A.L. Kagan, Phys. Lett. B **540**, 278 (2002) [hep-ph/0205274]
53. A. Kapustin, Z. Ligeti, Phys. Lett. B **355**, 318 (1995) [hep-ph/9506201]
54. Z. Ligeti, M.E. Luke, A.V. Manohar, M.B. Wise, Phys. Rev. D **60**, 034019 (1999) [hep-ph/9903305]
55. I. Bigi, N. Uraltsev, Int. J. Mod. Phys. A **17**, 4709 (2002) [hep-ph/0202175]
56. M. Beneke, A. Signer, Phys. Lett. B **471**, 233 (1999) [hep-ph/9906475]
57. S. Eidelman et al. [Particle Data Group], Phys. Lett. B **592**, 1 (2004)
58. V.M. Abazov et al. [D0 Collaboration], Nature **429**, 638 (2004) [hep-ex/0406031]
59. J. Charles et al. [CKMfitter Group], hep-ph/0406184
60. D. Cronin-Hennessy et al. [CLEO Collaboration], Phys. Rev. Lett. **87**, 251808 (2001) [hep-ex/0108033]; A.H. Mahmood et al. [CLEO Collaboration], Phys. Rev. D **67**, 072001 (2003) [hep-ex/0212051]
61. B. Aubert et al. [BaBar Collaboration], hep-ex/0307046; Phys. Rev. D **69**, 111103 (2004) [hep-ex/0403031]
62. B. Aubert et al. [BaBar Collaboration], Phys. Rev. Lett. **93**, 011803 (2004) [hep-ex/0404017]
63. F.M. Borzumati, C. Greub, Phys. Rev. D **58**, 074004 (1998) [hep-ph/9802391]
64. G.P. Korchemsky, G. Marchesini, Nucl. Phys. B **406**, 225 (1993) [hep-ph/9210281]

65. E. Gardi reports that he has confirmed (A.6) with $\kappa = 4/3$ from an independent calculation of the anomalous dimension $\gamma$ (private communication)
66. S.J. Brodsky, G.P. Lepage, P.B. Mackenzie, Phys. Rev. D **28**, 228 (1983)
67. M. Neubert, Phys. Rev. D **51**, 5924 (1995) [hep-ph/9412265]
68. F. Le Diberder, A. Pich, Phys. Lett. B **286**, 147 (1992)
69. O.V. Tarasov, A.A. Vladimirov, A.Y. Zharkov, Phys. Lett. B **93**, 429 (1980)
70. G. Korchemsky, private communication
71. A.K. Leibovich, I.Z. Rothstein, Phys. Rev. D **61**, 074006 (2000) [hep-ph/9907391]